Department of Electrical and Computer Engineering

Efficiency Improvements for Small-Scale Reverse-Osmosis Systems

Robertus B Susanto-Lee

This thesis is presented for the Degree of
Master of Engineering
of
Curtin University of Technology

November 2006

To the best of my knowledge and belief this thesis contains no material previously published by any other person except where due acknowledgement has been made. This thesis contains no material which has been accepted for the award of any other degree or diploma in any university.

Signature:

Name (printed): Robertus Budi Susanto-Lee

Date: 23/11/2006

To my wife Jennifer and my son Jordan,

may the world forever be a beautiful place.

Abstract

The water supplies of some small inland communities may come in the form of river systems that offer brackish water. Not fit for immediate human consumption, the water can be further processed using reverse osmosis to be converted into drinking water.

In very remote areas there are limited energy resources, and for those areas that lie beyond a municipal distribution grid, renewable energy sources may be used.

A reverse osmosis system that operates from the limited power generated by a renewable energy system must do so with the utmost of efficiency.

Three methods in improving the efficiency of small-scale reverse-osmosis system are investigated, namely high-pressure pump speed control, feed water heating and vacuum pump based energy recovery.

TABLE OF CONTENTS

LIST OF FIGURES

LIST OF TABLES

Chapter 1

1 INTRODUCTION

1.1 Context

The water supplies of some small inland communities may come in the form of river systems that offer brackish water. Not fit for immediate human consumption, this water requires further processing to be converted into drinking water.

Reverse osmosis filtration provides such a solution. The process of reverse osmosis is the highest form of water filtration in to date, removing all solids including metal ions and aqueous salts. A simple process, it is in essence the transmission of water through a filtration membrane by means of an electric pump. However, a lot of energy is required to facilitate this process.

Sourcing this energy is also an issue. In very remote areas there are limited energy resources, and for those areas that lie beyond a municipal distribution grid, renewable energy sources may be the answer. And where a renewable energy based power generation system is used, it is essential that the devices that utilise the generated power do so with the utmost of efficiency.

This observation forms the basis of this research, where new methods for improving the efficiency of small reverse-osmosis systems are the main objective. The preliminary objective however is no small task, requiring the construction of a reverse-osmosis system for the efficiency improvements to be implemented upon.

1.2 Project Objectives

The main objective of this project is to design and construct a small-scale reverse-osmosis desalination system. The building of this basic system will provide the foundation for the secondary objective, which is to perform tests on the proposed efficiency improvements. A functioning desalination system will also be a useful tool for future research projects, for further investigations into efficiency improvements and to perfect testing methods.

1.3 Achievements

The most significant achievement of this project is the construction of a desalination system, which includes a supervisory control system that enables close monitoring of the system's behaviour.

Also achieved in this project is a software model of the basic system, which was done in Matlab.

Steps to improve the efficiency of the system are also of considerable value, although due to the time constraints they are either not fully realised, or inconclusive.

1.4 Thesis Outline

In **Chapter 1**, the context of this project is offered to the reader, and the project's objectives and achievements are presented.

In **Chapter 2**, a brief background of the project topic is presented and the proposed efficiency enhancements are detailed.

In **Chapter 3**, the individual system components and their interconnection are detailed.

In **Chapter 4**, the control system programming is explained, detailing how the specified system control is implemented within the PLC and the HMI.

In **Chapter 5**, the system modeling method is detailed, and simulation results are analysed.

In **Chapter 6**, the experimental method is detailed, and the results are analysed.

In **Chapter 7**, conclusions about the project are discussed.

2 BACKGROUND

2.1 Reverse Osmosis

Reverse-osmosis is a water filtration method. It is referred to as hyper-filtration as it is the highest known form of filtration to date, removing all solids including metal ions and aqueous salts. This feature has made it one of the most popular forms of desalination. Today, reverse-osmosis is well represented throughout the world with units ranging from point of use units to municipal water supplies.

2.1.1 Basic Process

Osmosis is a natural process where a semi-permeable membrane allows water to pass from an area of high concentration, i.e. pure water, to an area of lower concentration, i.e. a water and solids solution (see Figure 2.1). Water will continue to flow in this direction until a pressure difference between the two areas is built up, preventing further flow of water. This pressure difference is called the *osmotic pressure* of the water and solids solution [1].

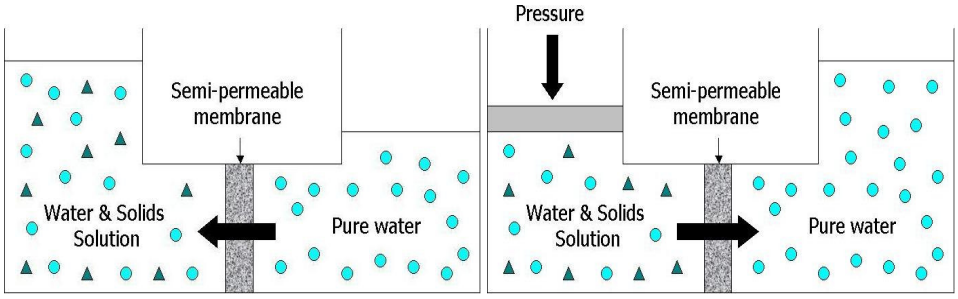

Figure 2.1: Osmosis (left) and Reverse-Osmosis (right)

At lower solution concentrations, this osmotic pressure can be determined using van't Hoffs's equation:

$$\pi = RT \sum X_i \qquad (2.1)$$

where

π is the osmotic pressure (kPa)
T is the temperature (K)
R is the universal gas constant, 8.314 kPa m^3/kgmol K
$\sum X_i$ is the concentration of all dissolved salts (kgmol/m^3)

Typical osmotic pressures at 25°C are shown in the following table.

Compound	Concentration (mg/L)	Osmotic Pressure (kPa)
NaCl	35,000	2744
Seawater	32,000	2344
NaCl	2,000	157
Brackish water	2,000 to 5,000	103 to 279

Table 2.1: Typical Osmotic Pressures

The osmosis process can be reversed however, by applying pressure on the water and solids solution. Providing that the pressure applied is higher than the osmotic pressure, pure water will flow through the membrane in the reverse direction (see Figure 1b). This process is called reverse-osmosis (RO).

2.1.2 RO Membranes

Reverse-osmosis is part of the membrane separations technology family, which also include, with respect to particle filtration size, microfiltration, ultrafiltration and nanofiltration. However, these three filtration methods use a sieving process whereby large (as compared to water molecules) waterborne particles are retained. Reverse-osmosis is different in that the sizes of the impurities are comparable to that of the water molecules. Hence the separation process must occur in the molecular realm, where passage selectivity is performed by the membrane's

chemical compatibility with water and its incompatibility with the chemical properties of aqueous salts. For example, cellulose acetate membranes have the chemical properties that allow the passage of water molecules whilst retaining salts. This is done through hydrogen bonds that form between the water molecules and the carboxyl groups of cellulose acetate. Cellulose acetate is one of the major types of commercial reverse-osmosis membranes, the other being composite polyamide.

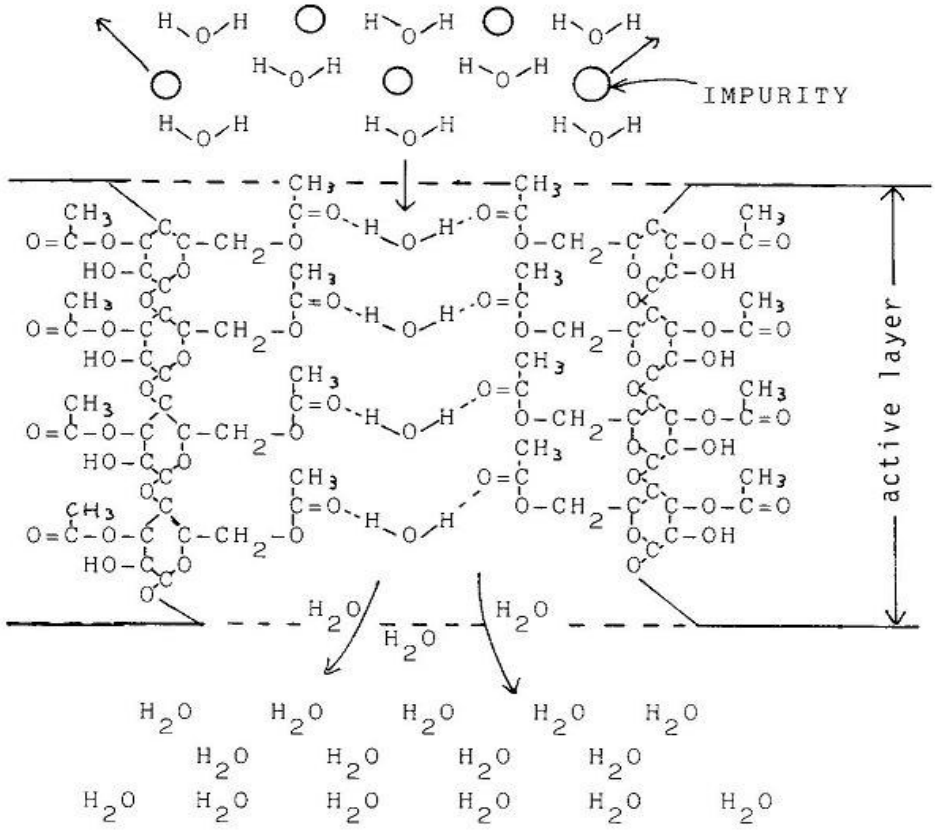

Figure 2.2: Reverse-Osmosis Chemical Process

RO membranes generally consist of a thin, dense, salt rejecting layer (1000-2000 Angstrom) and a porous support layer, to facilitate low salt passage and high

membrane flux (the superficial velocity of water through the membrane) respectively.

Figure 2.3 illustrates the general effects of applied pressure, feed temperature and water recovery on the membrane flux and water quality of reverse-osmosis membranes.

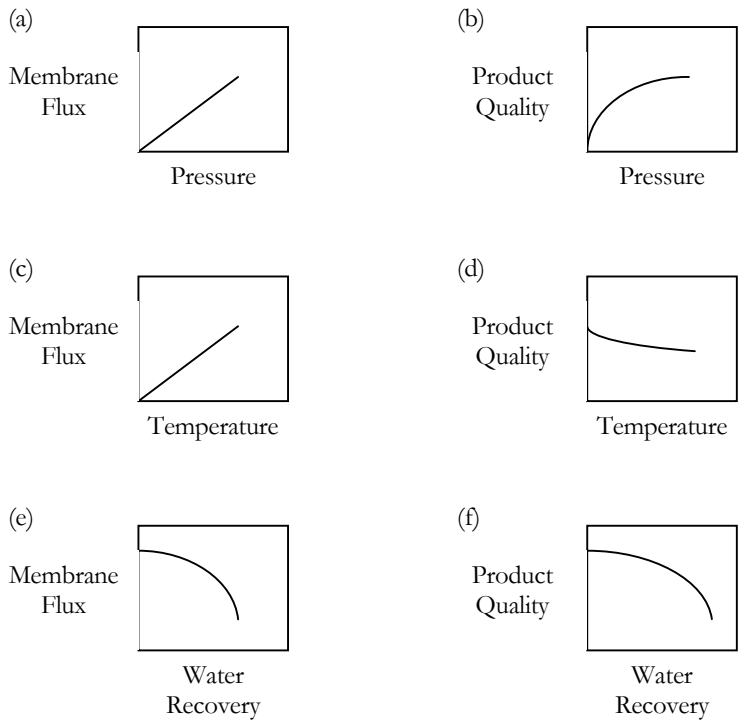

Figure 2.3: General Effects of Pressure, Temperature and Product Quality on Membrane Flux and Water Recovery

Membrane flux is proportional to the difference between the applied hydraulic pressure and osmotic pressures. It is also proportional to the membrane's permeability. It can be determined using Darcy's Law equation:

$$j_V = \frac{k}{L_c \mu} (\mathbf{\Delta} P - \sigma \mathbf{\Delta} \Pi) \quad (2.2)$$

where

j_V is the volumetric flux, L/m^2.day
$\mathbf{\Delta} P$ is the transmembrane pressure drop
σ is Staverman rejection coefficient (σ = 1 if 100% salt rejection)
$\mathbf{\Delta} \Pi$ is the osmotic pressure difference
k is the permeability constant
μ is the viscosity

Of particular interest to this project is the effect of temperature on the membrane flux; as the general trends in Figure 2.3 suggests, membrane flux rises proportionally to temperature. This is due to the effect of temperature on the feed water's viscosity. The viscosity of a liquid is inversely proportional to temperature, so as temperature increases, viscosity lowers, and according to equation 2.2, membrane flux will rise.

2.1.3 RO Membrane Modules

An efficient reverse-osmosis membrane must have a large surface area to enable a large amount of feed water to be processed. This is reflected in the design of reverse-osmosis membrane modules. The two most common module designs used in water desalination are the hollow fibres and the spiral wound modules.

Hollow fibres modules offer a very high membrane area due to the millions of individual hollow fibres used to permeate the product. Hollow fibres are made into bundles, and the feed solution flows on the inside of the fibres, in contact

with the dense salt rejecting layer. However, due to the fibre passage size these modules are quite susceptible to fouling by suspended matter in the feed solution.

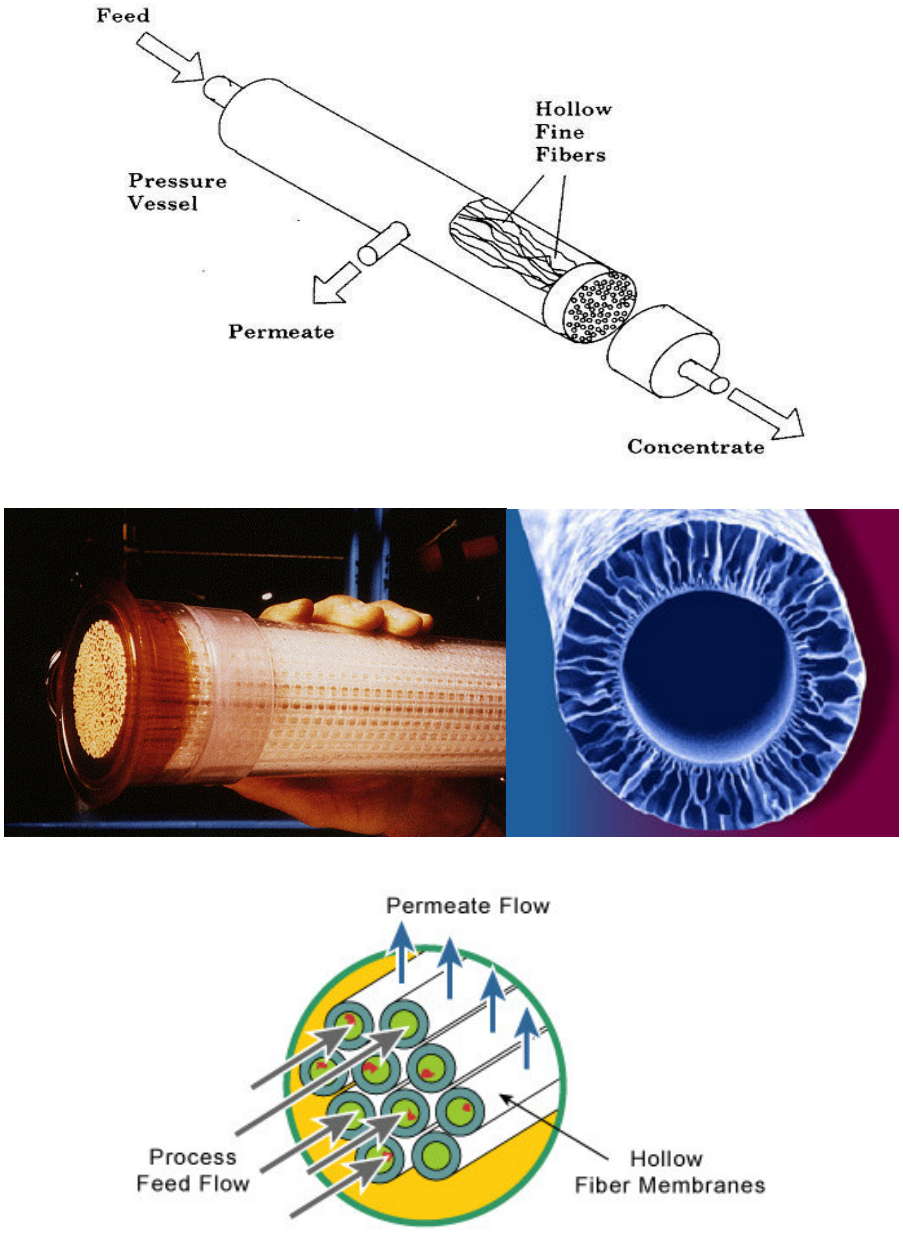

Figure 2.4: Hollow Fibre Membrane Module

Spiral wound modules also offer a large membrane surface area facilitated by two flat sheets of membrane separated by a permeate collector. A feed spacer material sheet is added and the assembly is wound around a perforated plastic permeate tube. This modules type is more widely used in industry largely owing to the fact that they are less susceptible to fouling.

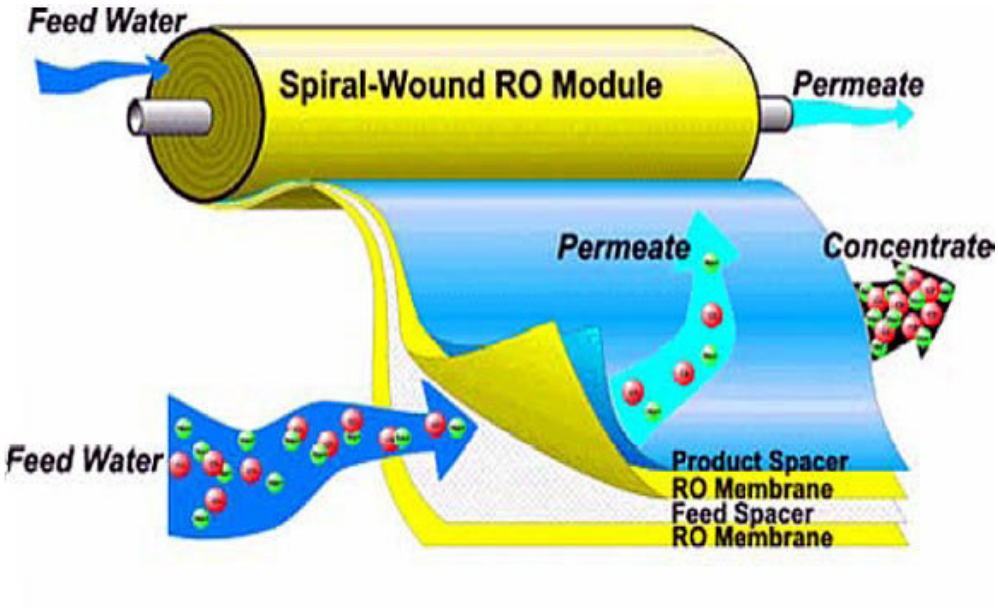

Figure 2.5: Spiral Wound Membrane Module

Water recovery is defined by the following equation:

$$\text{Recovery } (\%) = \frac{Volume_{permeated}}{Volume_{inlet}} \times 100 \qquad (2.3)$$

The recovery rate of a single module is low. To increase the water recovery, multiple modules (or multistage configuration) can be connected in a Christmas tree like array as shown in figure 2.6. Such configurations can have up to 90% recovery, and could dramatically reduce operating costs.

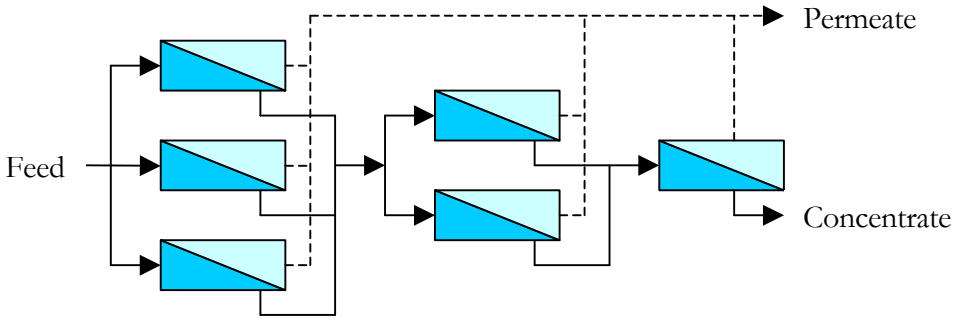

Figure 2.6: Multistage Reverse-Osmosis System

2.2 RO System Research

Figure 2.7 shows a simplified version a reverse-osmosis system. The feed water is input into the membrane at high pressure. The product water is the permeate water that has passed through the membrane and is output at a relatively low pressure. The brine is the doubly concentrated wastewater that is rejected by the membrane, which exits at a pressure only slightly lower than that of the feed water.

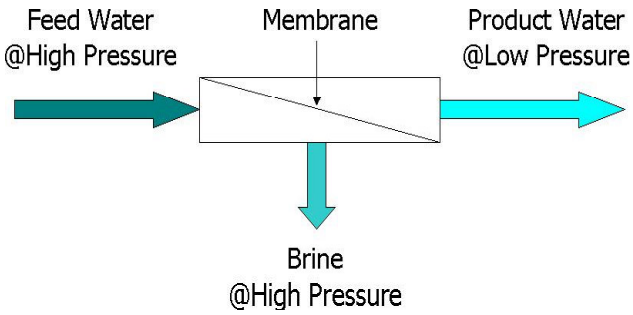

Figure 2.7: A simplified model of a reverse-osmosis system

The practical implementation of the reverse-osmosis process presents many challenges, some of which has launched numerous research projects. The commonly focused areas are as follows.

2.2.1 High Feed Pressure Production

High feed pressure production is of great importance in reverse-osmosis system research, as being the driving stage; it is the stage that consumes the most energy. There are a variety of ways to produce the required feed water pressure, some of which have been successfully implemented. A few innovative examples follow.

One elegant solution was the use of the available and renewable seawater and energy found in the sea at some depth [2]. A reverse-osmosis installation is transported to a depth of 600 metres below sea level. The water pressure this level is greater than the seawater's osmotic pressure, hence creating the force required to push permeate water through the membranes without any energy costs. An electrically driven low head pump would still be required to pump water to the onshore storage unit, but at a significantly lower energy demand overall.

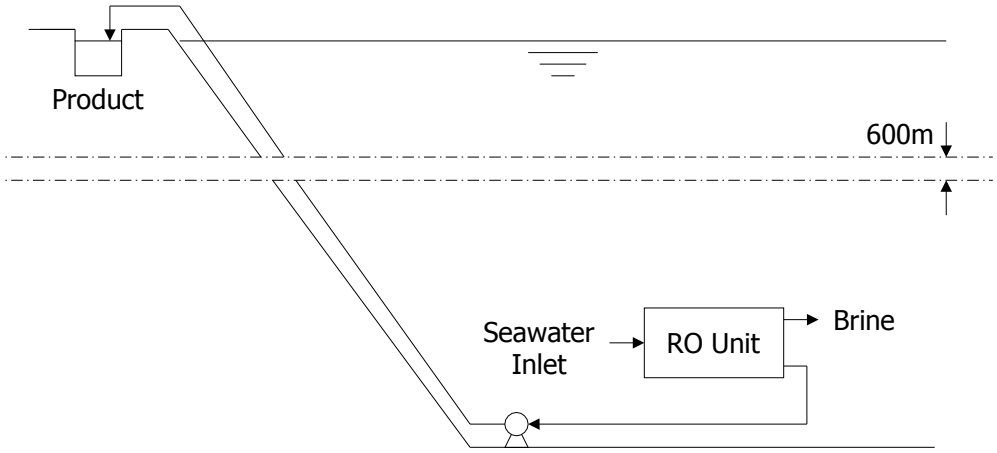

Figure 2.8: Deep-Sea Reverse Osmosis

Another novel method of creating raw water pressure is demonstrated in centrifugal reverse-osmosis [3]. Raw water is fed into a centrifuge rotor and high pressure is created by the centrifugal force that is developed inside the spinning rotor.

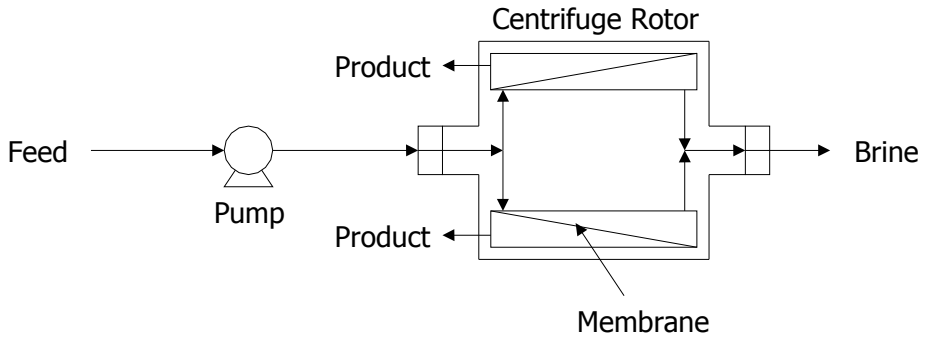

Figure 2.9: Centrifugal Reverse-Osmosis

These techniques are novel in that they exploit natural physical phenomena and may operate with improved efficiency, though their implementations present their own challenges.

However, the most common method in producing the high feed pressure is the use of pumps driven by electric motors, due to their availability and cost. The implementations of such systems are a known quantity in industry and their off-the-shelf availability makes it an attractive and safe option.

2.2.2 Improved Productivity via Membrane Technology

Other research has focused on lowering the pressure required by the development of ultra low-pressure membranes. Ultra-low pressure membranes is reported to have an almost 30% higher design permeate productivity than conventional membranes [4]. Such membranes would present a great energy saving as less energy would be required to produce required product flows.

2.2.3 Recycling Energy from the Brine Stream

In systems where high-pressure pumps have been employed, the brine stream exiting the membrane is expelled at a slightly lower pressure than the inlet pressure. A substantial amount of energy can be recovered from this brine stream via an energy recovery mechanism and reused, thereby increasing system efficiency.

The *pressure exchanger* is one such mechanism. It uses the high-pressure brine stream to pressurise the raw water by direct contact [5]. The pressure exchange occurs in the ducts of a rotor spinning at high speed. The output of this device can be further boosted to match the high-pressure pump pressure and fed directly into the membrane.

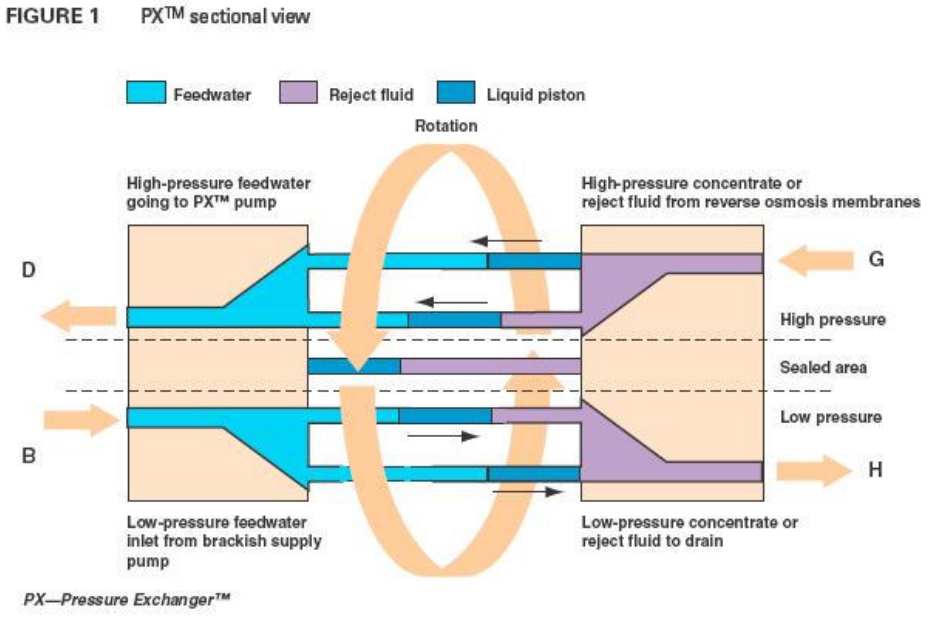

Figure 2.10: Pressure Exchanger

Another innovative design for an energy recovery device is the Clark pump. It takes a different approach to pressure exchange by using the brine stream to drive a reciprocating piston [6]. A series of valves control the water flow that enables the pressure exchange to occur.

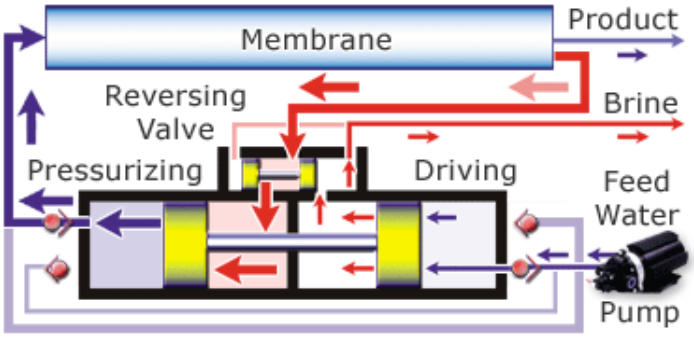

Figure 2.11: Clark Pump

A simple mechanism to harness the brine stream is the hydraulic motor, which converts the pressurised hydraulic energy into rotational kinetic energy, or torque. This torque can then be used to drive an electrical generator to convert the mechanical energy into electrical energy, which in turn is fed back into the high-pressure pump drive (see Figure 2.12). An alternative configuration uses the torque to mechanically assist the high-pressure pump motor (see Figure 2.13) [7].

(a)

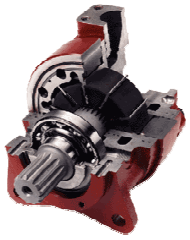

(b)

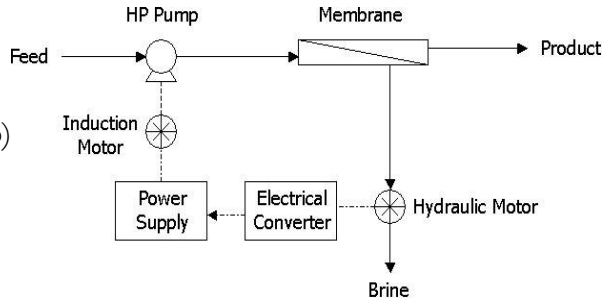

Figure 2.12: (a) Hydraulic Motor (b) Electrical Generator

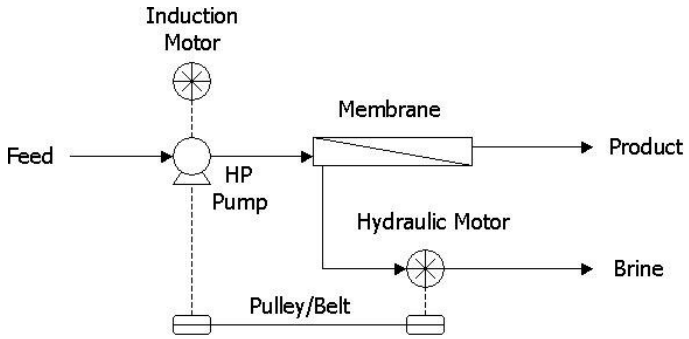

Figure 2.13: Torque generator

2.2.4 Process Control

The reverse-osmosis system requires instrumentation and a control system to monitor and control the process, such as monitoring feed and product water quality (conductivity, pH, turbidity), pressure and flow rates, tank levels, and controlling the feed pressure and controlling any chemical dosing based on flow.

As well as administering the basic process, the control system can also be used to control the amount of energy being used. In this project, an electric pump is used to produce the high pressure feed, and it represents the major consumer of energy in the system. The control system can control the speed of the pump, which in turn produces the pressure against the membrane. Hence two automatic pressure/flow control strategies will be compared, namely on-off control and PID control.

2.3 Proposed Efficiency Improvements

The three proposals in this research project are three original ideas motivated by three different issues, namely pump-motor life, productivity and energy recovery; the common theme being energy efficiency.

And to counter these issues are pump speed control, feed water heating and vacuum pump based energy recovery, respectively.

If any of these methods can be shown to effectively tackle the issues they are targeted for, they can be of significant value in improving the efficiency of existing systems. Assume that an existing system is as shown in Figure 2.14 below, and that the following proposed efficiency enhancements are to be implemented on this system.

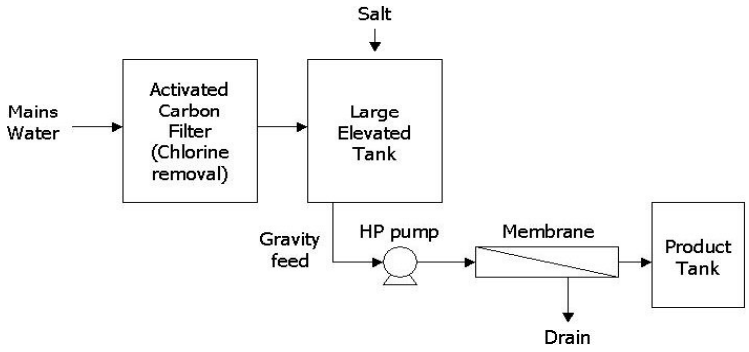

Figure 2.14: Basic Reverse-Osmosis System

2.3.1 Pump Speed Control

Repetitive motor starting and stopping shortens the life of motor control components such as starters, relays and capacitors, which in turn decreases pump-motor life. This is observed in the typical control logic used by most small reverse-osmosis systems. Essentially, the system is control by a set of level switches in the product tank. A low level will start the system, and a high level will stop the system. When the system is started the high-pressure pump is always run at 100% capacity. This control scheme allows the high tank level to be reached in times of low demand. In the hourly water consumption sample below, the low demand period starts at 10pm and ends at 6am the next day.

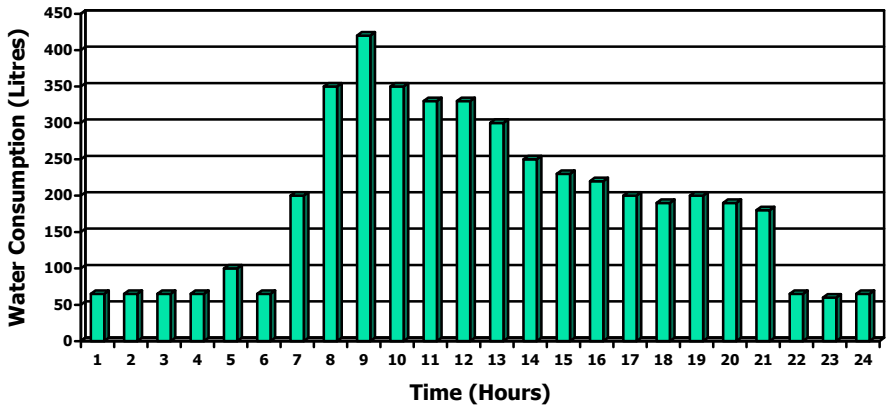

Figure 2.15: Hourly Water Consumption Sample

Using the abovementioned control scheme, the product tank may reach high level at around 4am, where the system would stop. To avoid this event, it is proposed that the speed of the pump is controlled in such a way that the product water level will be near high level when the high demand period starts again. This strategy will ensure that the pump will never be stopped unnecessarily, and that the water supply is kept at close to maximum. It is proposed that a PI (proportional-integral) controller be used for this purpose, using the tank-filling rate as the feedback variable.

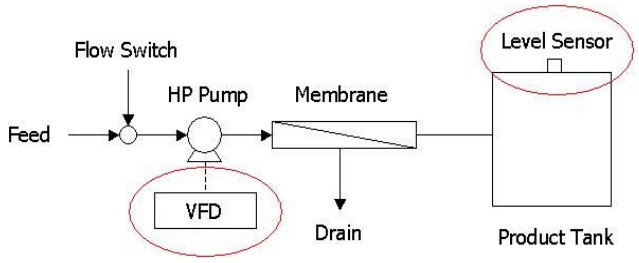

Figure 2.16: Pump Speed Control Test Scheme

The extra equipment required to implement this configuration on the existing system would ideally be a variable frequency drive (VFD) and a level sensor (see Figure 2.16). A controller is also required to input the level sensor readings and determine the automatic speed set point that is sent to the VFD. Note that this equipment is integrated into the design of the reverse-osmosis system that was constructed.

2.3.2 Feed Water Heating

Water is less viscous in higher temperatures. Where water is less viscous, a smaller amount of force is required to push it through a reverse-osmosis membrane. It is proposed that this physical property be exploited to increase productivity.

The only extra equipment to add on to the existing system to implement this test is a temperature sensor. It is proposed that when making a saltwater batch heated filtered water is used (see Figure 2.17). When the right temperature and salinity is achieved the efficiency tests can be performed.

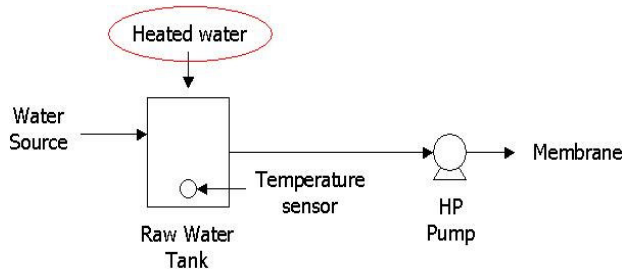

Figure 2.17: Feed Water Heating Test Scheme

2.3.3 Vacuum Pump Based Energy Recovery

This proposal is a new approach in using the recovered energy from the brine stream. Using a hydraulic motor as the energy recovery device, the torque produced is used to drive a vacuum pump on the product side of the membrane.

This vacuum pump may offer an increased pressure difference across the membrane, effectively 'pulling' pure water out of the membrane, as the high-pressure pump is 'pushing' water into membrane.

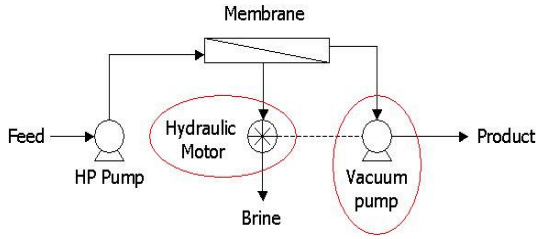

Figure 2.18: Vacuum Pump Test Scheme

The extra equipment required for this test is a hydraulic motor and a vacuum pump. The hydraulic pump will accept the brine from the membrane before going to the drain, to recover the hydraulic energy (see Figure 2.18). The torque produced by the hydraulic motor will be connected directly to a vacuum pump, which is connected on the product outlet side of the membrane.

3 SYSTEM COMPONENTS

The first part of this project will focus on the design and construction a simple reverse-osmosis system. A schematic of the system is as follows:

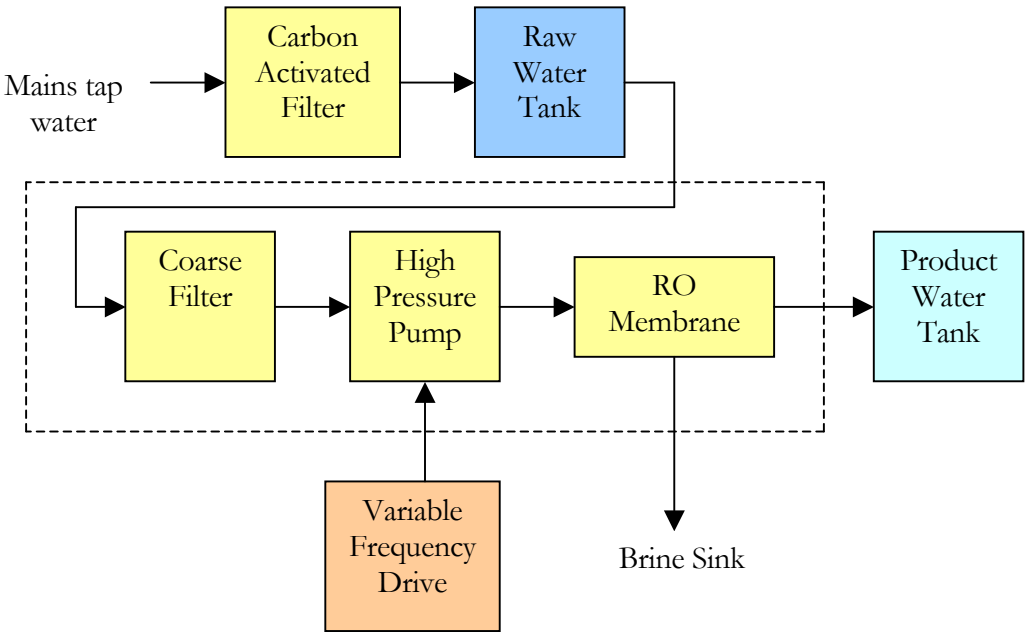

Figure 3.1: System Schematic

The components in the dotted line are part of a package system. Note that the first efficiency improvement proposal, namely high-pressure pump speed control, is integrated into the design by including the variable frequency drive.

Mains water is input into the system via a regulation tap directly piped to an Activated Carbon Filter. This filter is responsible for the removal of chlorine from the mains water, which can irreversibly damage the cellulose-based structure of the reverse-osmosis membrane.

The filtered water then flows into the raw water tank. This is where the water can be treated to simulate different salinity conditions. Note that this tank is elevated so that it is on a higher level to the reverse-osmosis desalinator package unit (desalinator), to take advantage of 'gravity feeding' into the desalinator. The water flow to the desalinator is controlled using a manual valve (like a tap).

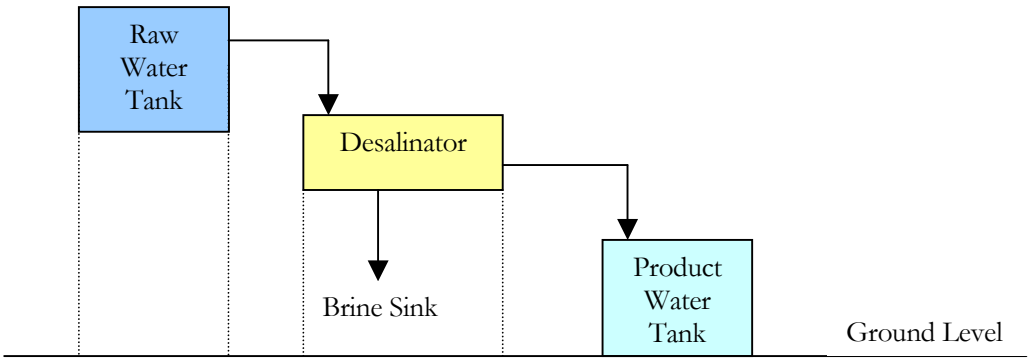

Figure 3.2: System Elevation Scheme

The desalinator consists of a cartridge filter, for the removal of large water-borne materials, a high-pressure pump, for pressurizing the water for the next stage, and a reverse-osmosis membrane. This spiral-wound membrane is encased in a tube that has one inlet connector and two outlet ports, one for the permeate or 'product water' and the other for the concentrate or 'brine' to be expelled. Approximately 15% of the feed flow into the membrane will pass through the product water port, and is piped into the product water tank. The remaining brine is piped into the sink.

The piping that interconnects the system modules are customised lengths of a normal household garden hose.

3.1 Reverse-Osmosis Desalinator Package Unit

This desalinator package unit comprise of a coarse filter, high-pressure pump and a reverse-osmosis membrane. It was purchased from Citor Pty. Ltd., a water purification equipment manufacturer in Fremantle, Western Australia. Citor offered several different models of compact desalinators. The model selected (1TM) was the smallest available off-the shelf reverse osmosis system for brackish water, with a production rate of 1000 litres per day at 25ºC.

Figure 3.3: Desalinator Package Unit

3.1.1 Cartridge Filter

The Cartridge Filter is the first filtration component of the desalinator package unit. It is a relatively coarse filter, designed to filter particles above 5 microns from the feed water. Replacement cartridges were supplied along with the desalinator. The clear housing allows operators to monitor the amount of fouling that will occur over time. This is apparent in the darkening of the colour of the

cartridge. Ensure to replace the cartridge when required, as clogging will cause the pump to take in air through the joints and threads. This will cause the pump to run roughly.

Figure 3.4: Cartridge filter

3.1.2 Three-phase Motor

Upon request, Citor also modified the base model desalinator to install in place of the existing single-phase AC electric motor a three-phase AC electric motor, so as to accept supply from the variable frequency drive.

This motor is a waterproof insulated three-phase 4 pole induction motor (CMG SLA), 415V, 50 Hz, 0.37 kW.

Figure 3.5: AC induction motor

The power terminals were delta connected, giving 220-240V per phase.

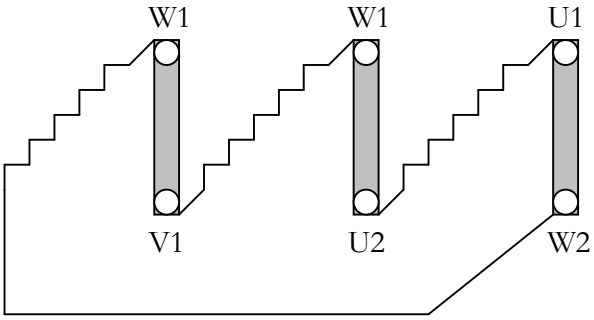

Figure 3.6: Power terminal delta connection

3.1.3 High Pressure Pump

The installed pump is a Fluid-o-Tech Rotoflow PO500 high volume rotary vane pump, which operate with consistent performance and stability at low pressures. Its flow rate ranges from 500 to 1000 litres per hour at 1450 rpm. The maximum pressure that can be delivered is 1600 kPa.

(a)  (b) 

Figure 3.7: (a) Rotary vane pump (b) motor-pump installation

3.1.4 Membrane

This desalinator unit features a DOW Filmtec TW30-2521 membrane, which can operate at 99% salt rejection at very low applied pressure. It is a spiral wound membrane and is a type of polyamide thin-film composite. The membrane is located within the desalinator frame.

Items of the membrane specification	Constraints
Max Permeate	1400 litres/day
Maximum Operating Temperature	$113^0 F\ (45^0 C)$
Normal Operation recovery ratio	15%
Maximum Operating Pressure	600 psi (41bar)
Operation pressure	0-25 bar
PH Range continuous Operation	2-11
Free Chlorine Tolerance	<0.1ppm
Salt rejection	99%

Table 3.1: Specification of the RO membrane

Figure 3.8: Membrane in desalinator frame

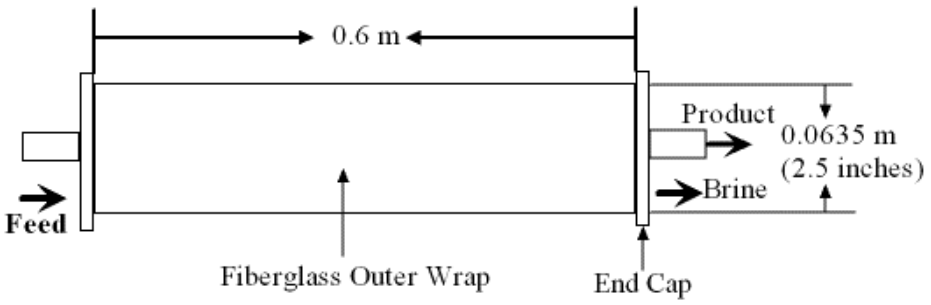

Figure 3.9: Membrane compartment dimensions

Membranes are sensitive to overpressure and oxidation. For correct and long-life operation, consult the operation and maintenance document in appendix Z.

3.1.5 Operation Switch and Pressure Meter

The desalinator has an operation switch has 3 settings: Off, Start and Operate. The operation switch is essentially a valve director; when set to Start, water is pumped straight to the drain pipe; when set to Operate, water is pumped into the membrane.

(a) (b)

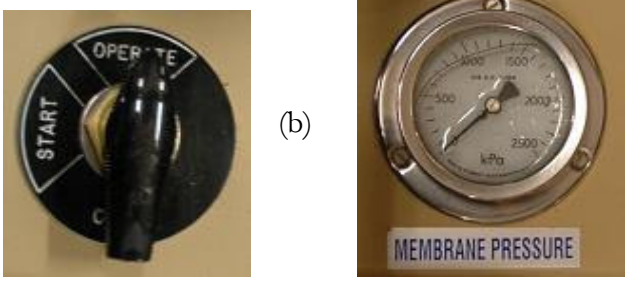

Figure 3.10: (a) Operation switch (b) Pressure meter

A pressure meter is installed on the desalinator to enable operators to monitor the differential pressure between the inlet and outlet of the membrane.

3.1.6 Activated Carbon Filter

Also purchased from the same vendor is the Activated Carbon Filter. The installation of this filter before the desalinator is essential when using water from a mains source by removing the high chlorine content of the water. This filtering will protect the reverse-osmosis membrane from irreversible damage, as high levels of free chlorine will chemically react with the membrane material.

The filter media is a deep bed of activated carbon, which is a highly adsorbent material with a very high capacity for the removal of tastes/odours, chlorine and Trichlormethane. The filter media is held within a cylinder; it sits on top of a gravel bed and a centre tube passes through the media. Normal service flow is down through the filter bed and back up the centre tube. During backwashing, the flow is reversed flushing sediment out of the filter bed.

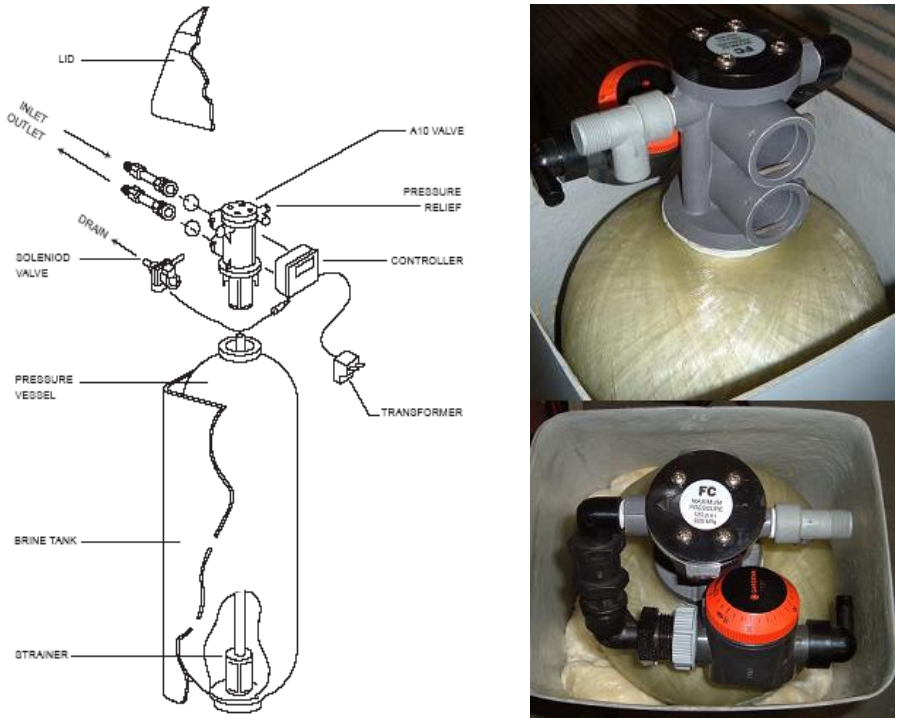

Figure 3.11: Activated Carbon Filter assembly

3.2 Tanks

Two tanks, namely the raw water tank and the product water tank, were used in the project. They were both supplied by Curtin Electrical Laboratory.

3.2.1 Raw Water Tank

The raw water tank has a capacity of approximately 315 litres and is used to store what would be the raw feed water. In this system it receives filtered water from the activated carbon filter, which is relatively free of chlorine and salt. This is where the water salinity can be simulated, by adding salt into the tank to achieve a desired concentration. The treated water is inlet into the desalinator via a manual valve and in turn allowing water to be drawn by the desalinator pump.

(a)  (b) 

Figure 3.12: (a) Raw water tank (b) Product water tank

3.2.2 Product Water Tank

The product water tank has a capacity of approximately 200 litres and is used to store the RO membrane 'permeate', or product water. This is the drinking water

storage area produced by the system. Consumers can draw clean drinking water from this tank.

3.3 24VDC Power Supply

The devices that require power, such as the system controller (PLC) I/O cards and the frequency converters need a 24VDC source. A single-phase switch-mode power supply was installed to satisfy this requirement. It accepts a 240VAC, 50Hz input (from mains power) and it delivers a reliable 24VDC up to 5A. The 120W capacity is ample for the 24VDC requirements of this system.

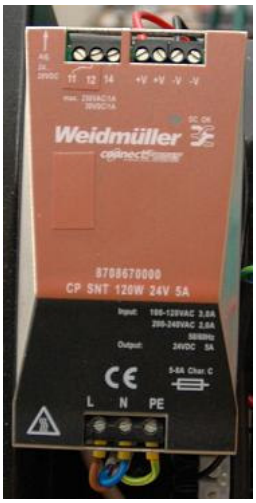

Figure 3.13: 24VDC power supply

3.4 Programmable Logic Controller (PLC)

A Programmable Logic Controller (PLC) is installed to act as the system controller. The installed PLC is Koyo DL205 PLC, donated to the project by Tenix Alliance, Burswood WA. The main feature of a PLC is that the control logic can be easily programmed and modified via a programming device (usually a PC), making it a flexible and powerful tool. It also has a modular approach to

input and output (I/O) hardware, which enables the user to configure and customise the system I/O to the application.

The base of the PLC is a back-plane with a built-in power supply. The power supply accepts 240VAC, 50Hz input (from mains power) and supplies 24VDC to the system. This back-plane contain the slots onto which the other modules are connected to.

Figure 3.14: Programmable logic controller (PLC)

Slot	Module	Description
-	D2-06B-1	DL205 6 slot back-plane and 110/220VAC power supply
1	D2-260	DL260 CPU (with built-in PID loop capability)
2	D2-16ND3-2	16 channel 24VDC digital input module
3	H2-ECOM	Ethernet module
4	F2-08AD-1	8 channel 4-20mA analog input module
5	F2-02DA-1L	2 channel 4-20mA analog output module
6	D2-08TR	8 channel relay output module

Table 3.2: PLC configuration

The installed modules include a Central Processing Unit (CPU), an Ethernet communications module, and I/O modules. The CPU is where the program logic is stored and executed, and it is the module that a programming device connects to for downloading program logic. The Ethernet module enables Ethernet communication from a programming device and/or an HMI (Human Machine Interface) to the PLC, by means of an Ethernet cable. The I/O modules are used to facilitate the monitoring and control of the process plant. The CPU gathers the required information from the I/O modules via a bus on the back-plane.

The above figure and table show the slot-module allocation for the RO system.

Note that the I/O modules (digital input, relay output, analog input and analog output) require 24VDC and are supplied by the 24VDC power supply (see section 3.3).

The PLC is programmed using DirectSoft32 PLC programming software. This software was loaned to the project by Bloch Technologies. In this project, this programming software is run on the HMI PC, hence this PC is the PLC programming device. PLC logic monitoring, modification and whole program downloads to the PLC are done over the same Ethernet link that the HMI uses for its data acquisition.

3.5 Single-Phase to Three-Phase Inverter (Variable Frequency Drive)

A 1kW single phase to three-phase inverter was made available for use in this project by Curtin Electrical Laboratory. It is an all-digital, mini size inverter (TECO Speecon 7200J) that converts power from single phase AC to three-phase AC. It powers the motor-pump of the desalinator (which is rated at 0.37kW). The inverter is used to vary the speed of the pump. A block of terminals on this device facilitates communications to a remote controller. An analog input terminal accepts a speed reference and a set of digital terminals

accept start/stop signals. These signals come from the PLC - an analog output channel and a pair of output relay channels respectively. It also has an RS-485 communications port, which can provide serial communications to a remote controller, but it was not used for this project.

Figure 3.15: Inverter

The front panel of the inverter allows the operator to configure the inverter as required. The configuration of the inverter is as follows:

Parameter	Setting	Description
01	3	Control via terminals
28	110	Frequency upper limit
36	0	3-Wire (A) sequence connection
81	1	Analog frequency reference
82	1	4-20mA

Table 3.3: Inverter configuration

The remaining parameters can be left as defaults. Please refer to Appendix C for more information on parameters.

3.6 System Instrumentation

System instrumentation was installed to monitor the system's operational statistics, such as water flow, water quality and tank levels. All of these devices interface to the PLC (see section 3.4), hence it was a prerequisite that they have the correct signal formats. Digital input and output devices derive their potential difference or signal supply from the PLC itself; hence they are not an issue. However, analog signal devices do not rely on outside sources for signal generation or detection, so it is essential that its signal format match that of the PLC's analog input or output module. The PLC's analog input and output modules are 4-20mA; hence all instruments that interface the controller are required to be 4-20mA.

3.6.1 Flow Sensors

Flow sensors are installed at the inlet and the outlet of the product water tank. Due to the absence of an ultrasonic level transmitter to detect the water level in the product water tank, water demand is calculated by monitoring the difference between these two flows.

Figure 3.16: Flow sensor

These flow sensors were sourced from RS Electronics. They give a pulse output, the frequency of which is proportional to the flow rate through the device. A lower flow rate range is achieved by inserting a restriction jet in the entry port of

the sensor. The specified flow range is 0.05 to 9 litres per minute, which is well above the operational flow rates of the system.

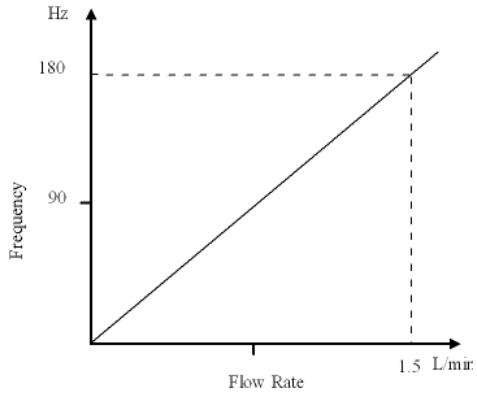

Figure 3.17: Flow sensor characteristics

3.6.1.1 Frequency to Analog Signal Converter

The pulse outputs are required to be converted into analog signals to be input into the PLC for monitoring. The Curtin Electrical Laboratory supplied two such conversion devices, one being a frequency to current converter and the other a frequency to voltage converter.

(a)

(b)

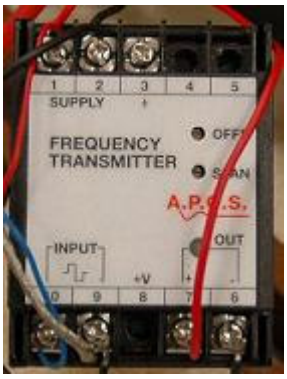

Figure 3.18: Frequency converters (a) to current (b) to voltage

The green Pepperl & Fuchs frequency converter is a fully configurable unit, to measure either frequency or speed, converted to either a voltage or current output. For this system, the configuration is as follows.

Parameter	Setting	Description
Func	0	Frequency measurement
Deci	1	Range 0-999.9
FrHi	200	Max Freq 200Hz
Outp	3	Output 4-20mA
FdSp	0	Display in Hz

Table 3.4: Pepperl & Fuchs frequency converter configuration

As previously mentioned the PLC only accepts current analog signals of 4-20mA. Hence the frequency to current converter is ideal, enabling direct connection to the controller. On the other hand the frequency to voltage converter requires further signal conditioning to convert the 0-10V voltage signal to a 4-20mA current signal. A voltage to current converter was required.

3.6.1.2 Voltage to Current Converter

Sourcing the voltage to current converter proved a challenge, as it was one of the few test instruments that the Curtin Electrical Laboratory did not stock. Commercial frequency to current converters start at around AUD500, which the project funds would scarcely cover. After much searching and deliberation a voltage to current conversion chip was eventually purchased online (from eBay).

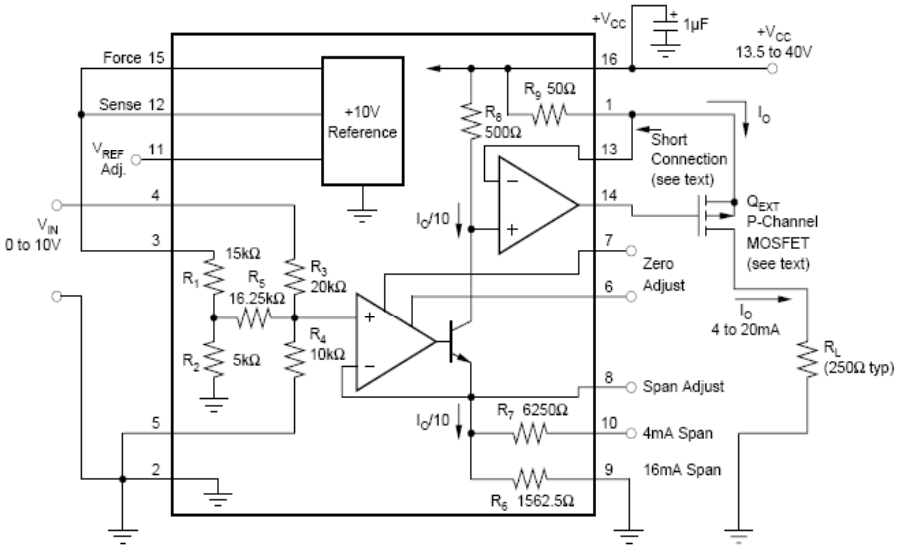

Figure 3.19: Voltage to current chip configuration

The chip was wired as shown in figure 3.19 on a breadboard and tested. Upon satisfying the conversion requirements, it was the transferred onto perfboard and encased in a small plastic box to slightly enhance its permanence and durability.

(a) 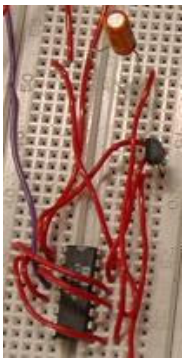 (b) 

Figure 3.20: V/I converter chip (a) on breadboard (b) on perfboard

3.6.2 Conductivity/Temperature Meter

Figure 3.21: Handheld conductivity/temperature meter

A conductivity meter is used to determine the salinity level in a body of water. This meter is primarily used when adding salt into the raw water tank to simulate a certain salt concentration. It consists of a meter and a probe. The probe is submerged in the water and a reading (in millisiemens per cm) is taken when the conductivity meter has stabilised.

The sourcing of this device also proved quite a challenge. Units were loaned to the project by the Water Corporation and Endress & Hauser, however only at short intervals. Eventually a handheld unit was sourced at Curtin Chemistry Laboratory, for loan on a daily basis (returned each day).

All the loaned units offered a temperature measurement mode, which enables the measurement of water temperature. This function is used to determine if the system is operating under specific conditions, particularly to carry out system productivity tests under different raw feed water temperatures.

3.6.3 Energy Consumption Meter

A Fluke 43B Power Quality Analyser was made available for use by the Curtin Electrical Laboratory. This device was used to monitor the instantaneous power flow drawn by the motor-pump, and to totalise power with respect to time and determine energy consumption over the testing period.

The meter has an accompanying software application, which was installed on the HMI PC. This software allows the monitoring and trending of various energy consumption data. This data can in turn be saved on the PC for later analysis.

The meter was connected to the HMI PC via an optical RS-232 data communication port on the meter, and the standard 9-pin RS-232 serial port on the HMI PC.

Figure 3.22: Energy consumption meter

3.7 Product Water Level Switches

Level switches are installed in the product water tank and the digital signals are returned to the PLC. These switches are supplied by Curtin Electrical Laboratory.

(a)

(b)

Figure 3.23: Level switches (a) high (b) low

3.8 Product Water DC Pump

Figure 3.24: Product water DC pump

A product water DC pump is installed in the product water tank in order to simulate a product demand for the system, to monitor how the programmed control strategy will perform under various water demand conditions over a certain period. The pump accepts a variable DC voltage to vary its speed. In this project however, a relay output of 24VDC from the PLC turns this pump on and off at approximately 8.4 L/m. The demand simulation program varies the demand by changing the on-time of the pump and the frequency of the on-times.

3.9 Human Machine Interface (HMI)

A Human Machine Interface (HMI) is typically a process control application software running on a personal computer (PC). Whereas the PLC is the device that interfaces with the field instruments, the HMI is the device that interfaces with the operator (or user). The PC is connected to the PLC via a communications link (Ethernet in this case).

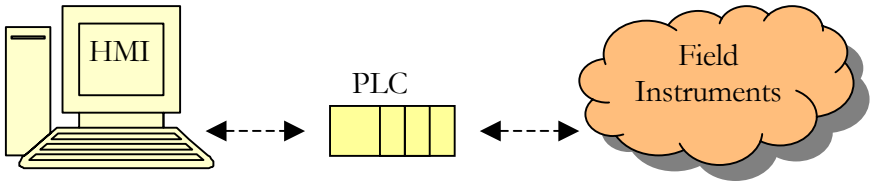

Figure 3.25: SCADA scheme

The HMI is used to aid in process visualisation and allows the monitoring and control of the process. This process control by means of an operator interface is also known as Supervisory, Control and Data Acquisition, or SCADA. Control functions such as starting pumps and manually setting an inverter's output frequency can be done through an on-screen pushbutton or direct set-point entry respectively. Process alarms such as pump faults and low flows can be displayed and logged for later analysis of faults or events. Analog values such as tank levels and flows can be monitored over a period of time by using trend charts.

Citect SCADA HMI version 5.2 is the process control application software used in this project. Licensing is controlled by means of a dongle, purchased from Citect, at a cost based on the desired I/O count size. The software and dongle was loaned to the project by Bloch Technologies. Below is a screen shot of the Citect project at runtime.

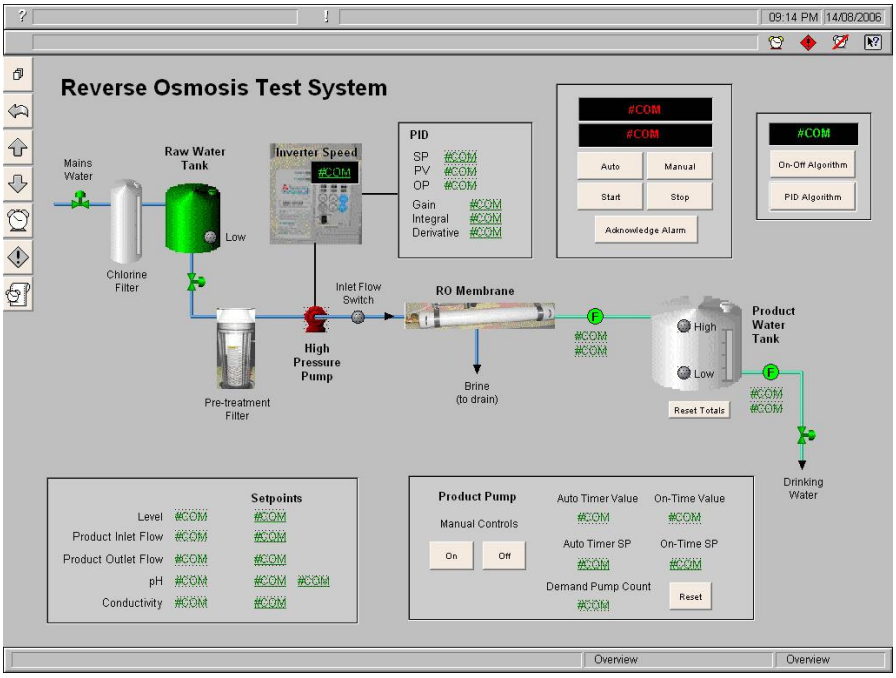

Figure 3.26: Citect runtime screenshot

Figure 3.27: HMI PC and Citect dongle

4 SYSTEM CONTROL

In any industrial process, a control system is required to monitor and control the process flow according to a functional specification and where possible maximise the process efficiency.

The core function of this system is the high-pressure pump control. On-off control is one of the most commonly used techniques in control systems because it is easy to implement and cheap to run. This control strategy is largely used in the systems that use storage equipment, especially water tanks. The essence of this control strategy is simply thus: a storage tank is equipped with a high and low level switch, which starts and stops a pump respectively. This control technique is considered simple but inefficient, in that in may continually start and stop the pump, increasing wear on the drive hardware.

An alternative control strategy is to adjust the pump speed in response to the demand. The main aim of this control strategy is to reduce starting and stopping of the pump and reduce the power usage where demand is low, and ultimately to increase the overall system efficiency. This approach may be implemented via a PID controller, a widely used software controller in process control systems.

These two strategies are implemented in the project's control system, in an effort to compare their efficiencies. The control system consists of a Programmable Logic Controller (PLC) and a Human Machine Interface (HMI). The following section will first detail the control system's functional specification, followed by the configuration of the PLC and HMI.

4.1 Functional Specification

The process is essentially the pumping of raw water through the RO membrane into the product water tank. Only one device, the high-pressure pump, is required to be controlled.

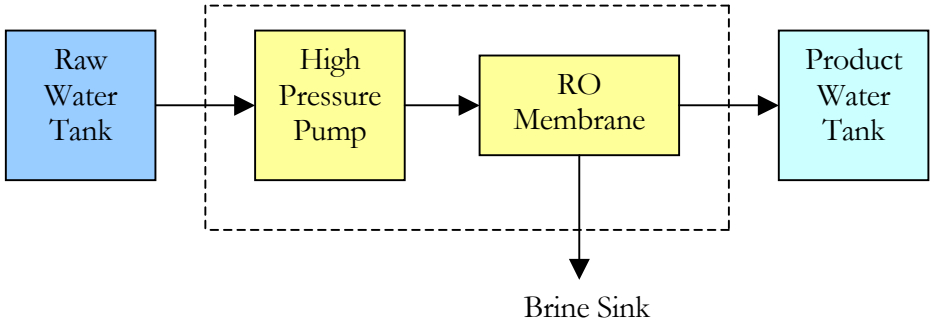

Figure 4.1: A simple process overview

Two methods of controlling the high-pressure pump will be available for selection, namely:

1. On-Off control
2. PID control

The On-Off control will monitor the product water tank level switches. When the low level switch is active, the water level in the product tank is low, and the pump is started at a constant frequency of 50Hz. When the high level switch is active, the product tank is full, and the pump is stopped.

In the PID control method, the pump is also started when the product tank low level switch is active. The system will monitor the water flowing in and out of the product water tank. The difference between the two flows, inflow minus outflow,

is input into a PID controller, and the PID output is used to control the pump speed. The PID setpoint should be set at 0, so that:

- If the difference is negative, increase the pump speed
- If the difference is positive, decrease the pump speed
- If there is no difference, maintain the current pump speed

The start-up frequency is set to be 20 Hz, which prevents motor from stalling. The highest frequency is set to be 65Hz. When the product tank high level switch is active, and the pump is stopped.

To test the performance of the above control methods with respect to energy efficiency, the control system is also used to simulate the product water demand. This is done by pulsing on and off a fixed speed pump in the product water tank. The duration and frequency of the pulses are varied to simulate different demand conditions.

The control flowchart of the system is as shown in Figure 4.2.

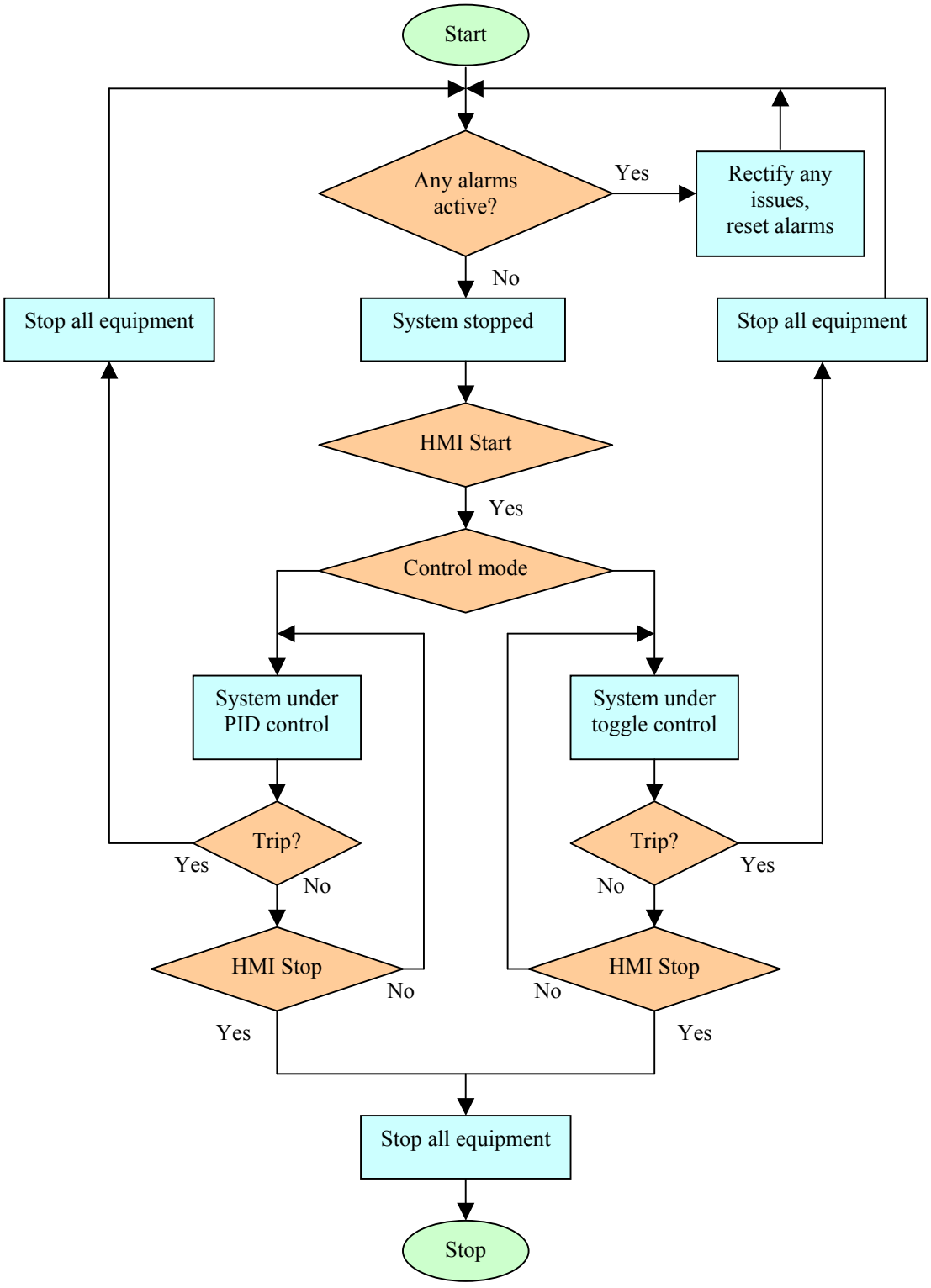

Figure 4.2: Control Flowchart

4.2 PLC Program

The implementation of the functional specification is done in a PLC program. It is programmed in ladder logic, which uses switch or relay contacts to realise Boolean expressions (AND, OR, etc). This program is downloaded into the PLC, which then interfaces the programmed logic with real world inputs and outputs. Where 'rungs' are referred to in following text, they refer to the PLC program printout found in Appendix A.

4.2.1 First Scan Configuration Logic

This first scan configuration logic (rung 1) is used to configure the PID controller when the PLC is first started (first scan). This allows the PLC to set aside resources that are required for the PID controller. Note that the CPU (DL260) was selected primarily as it supported 16 PID loops; lower models in the Koyo DL205 CPU range do not support PID loops.

4.2.2 Signal Monitoring

Analog signals are monitored via the logic in rungs 3 to 11. This section reads in 8 analog inputs. Rung 3 loads the value VX20 into the accumulator. VX20 holds the current value of the analog input card. Each of the inputs are continuously read in order, one per PLC scan, hence at any one scan only one analog input channel is read. The relay logic in rungs 4 to 11 represent the definition of the 3 bits (corresponding to 8 channels) that are used by the analog input card to determine which channel is being read at any time. The raw analog signals (12-bit resolution, decimal range 0-4095) are read in and stored in V-memory locations.

Digital inputs can be immediately accessed via bit memory octal addresses, preceded with the letter X. Outputs have a similar treatment, the only difference being that they are preceded by the letter Y. In rungs 17 to 21 digital input statuses (X bit addresses) are transferred to C addresses. C addresses are PLC

internal bit memory, which are used for PLC logic only and do not refer to real world inputs or outputs. In this case the values are transferred to them so that the HMI may in turn read the values from them. The may be read straight from the X bit memory, however it is good practice to transfer them into internal bit memory, in case some logical signal conditioning is required to be added in the future (e.g. inversion, timers).

4.2.3 Flow Scaling and Totalisation

For the two product tank flow meters (inflow and outflow), 2 different types of frequency converters were used. These frequency converters output 4-20mA signals, but of different ranges. Hence the raw analog input values need to be scaled to their respective intended ranges, as seen in rungs 45 to 56. The inlet flow range is 0.00 to 1.60 L/min and the outlet flow range is 0.00 to 16.76 L/min. These flow are converted to litres per second by further dividing them by 60. This L/s value is accumulated every second to give a running flow total. The flow totals can be reset via a signal from the HMI.

4.2.4 Fault Latching

Critical faults will be latched on until they are reset, and this is implemented via the logic in rungs 23 to 26. If the high-pressure pump contactor does not close in 5 seconds, detected by a contact relay, the high-pressure pump may be faulty and a high-pressure pump fault is latched. Similarly if there is no flow detected by a flow switch after 10 seconds, there may be a blockage in the system and a no flow fault is latched. Only an alarm acknowledgement request from the HMI will reset these faults. However, the aforementioned switch devices were not acquired in time for project testing and were considered low priority due to the system size. As a result the fault latching logic was disabled by adding an SP2 contact in the rungs, a PLC internal bit which is always inactive, to ensure that none of these fault signals can be generated at any time.

4.2.5 Pump Control

The control logic that starts and stops the pump is found in rungs 13 to 15. The pump can be started by the operator via the HMI when in Manual mode, and it may also be started by the system automatically when the product tank low level switch is active when in Automatic mode. The pump can be stopped by the operator via the HMI when in Manual mode. In addition to this, an array of system conditions and faults may stop the pump at any time, in any mode. The most significant of these is the product tank high level switch active signal, being a necessary precaution against overflowing the product tank.

Other control logic concerning the pump such as control mode selection and speed control are detailed in the following sections.

4.2.5.1 Mode Selection

The control logic that enables to operator to select the control mode of the pump is found in rung 36. Buttons for mode selection are available on the HMI. When the operator clicks on the Manual mode button, an internal bit address is set to 0 to signify that manual mode has been selected. When the Auto mode button is clicked, the same internal bit is toggled to signify that automatic mode has been selected. This internal bit is in turn used elsewhere in the program logic as a logical condition.

4.2.5.2 Algorithm Selection

When the pump has started and is operating, there are two ways of controlling its speed, namely on-off control and PID control. The logic used to select between these two algorithms is found in rung 28. Buttons for algorithm selection are available on the HMI. When the operator clicks on the on-off control button, an internal bit address is set to 0 to signify that algorithm 1, on-off control, has been selected. When the PID control button is clicked, the same internal bit is toggled

to signify that algorithm 2, PID control, has been selected. This internal bit is in turn used elsewhere in the program logic as a logical condition.

4.2.5.3 On-Off Control

On-off control was essentially implemented in the pump start-stop logic, in rungs 13 to 15. The pump would start when the product water tank was low, and it would stop when the product water tank is high. The only extra logic for this control algorithm is the setting of the pump speed when it is started. This is done in rung 42, where if the pump is in automatic mode and on-off algorithm has been selected, the pump speed (motor frequency) is set to 50Hz.

4.2.5.4 PID Control

As mentioned above the PID loop is initially configured by the first scan logic (see 4.2.1 First Scan Logic). The PID loop's mode registers (V3000, V3001) were assigned configuration values that essentially configures a closed loop PID controller (see Appendix E), with an output low limit of 20Hz. The process variable input of the PID loop is defined in rung 30. The process variable is the difference between scaled values of the product water inlet and outlet flows (in L/s) multiplied by 100 and added by 2048.

$$PV = ((\text{Inlet flow} - \text{Outlet flow}) * 100) + 2048$$

As the PV value input into the PID controller is required to be in 12-bit format, which has a resolution of 0 to 4095, a middle value is used as the zero point, which is 4096/2 = 2048. This is so that for negative values of the PV, where the outlet flow is greater than the inlet flow, would also be processed by the PID controller. The setpoint of the PID (written directly from the HMI) is set to 2048, and the error will be an offset of this value. Hence when the error is negative (outlet greater than inlet) and the PV is less than 2048, the PID controller will increase its output; when the error is positive (inlet greater than

outlet) and the PV is greater than 2048, the PID controlled will decrease its output.

As the inlet and outlet flow values tended to be within the 0.01 to 1.50 range, to register a significant error the PV is multiplied by 100. Note that changing this multiplier value is in effect changing the PID controller's proportional gain, and the same result may have been implemented by changing the PID controller's gain value. However the limiting factor was the PID controller's 12-bit resolution, which meant that if the error value were less than 1/4096, it would not be sensed by the PID controller. The value of 100 was essential in increasing the order of the error over this threshold.

Rungs 37 and 38 puts the PID controller into auto or manual. In auto, the PID will work as described above, whereas in manual, the operator can specify an output value for the PID controller.

It was also observed during testing that the analog input span of the Teco VSD was 173 to 3880 to represent 0-65Hz, as opposed to using the entire 12-bit range of 0-4095. Hence an offset and a scaling factor were required when converting from the desired frequency to the VSD input value, as can be found in rungs 40 and 41.

Also observed during testing that the process variable can be very erratic, which made a high gain PID loop behave rather undesirably. Some signal filtering as seen in rungs 31 and 32 was included to smooth out the signal. This is done by scanning the process variable every 5 seconds instead of every PLC scan, which is in the order of milliseconds.

4.2.6 Product Pump Control and Demand Simulation

The product pump in the product water tank is controlled by the logic found in rungs 57 to 65. When the pump is in Manual mode, the operator can start and stop the pump from the HMI. When the pump is in Automatic mode, the pump is controlled by the demand simulation logic. The demand simulation logic uses two counters. The first counter is the 'off' counter, which governs the length of time between pump operations (intervals). The second counter is the 'on' counter, which governs the length of time that the pump is run; this counter is set to 20 seconds. Thus the demand simulation logic will run the pump for 20 seconds every specified interval. This interval can be varied to simulate different demand loads.

A typical small community water consumption chart is produced as shown in Figure 4.3.

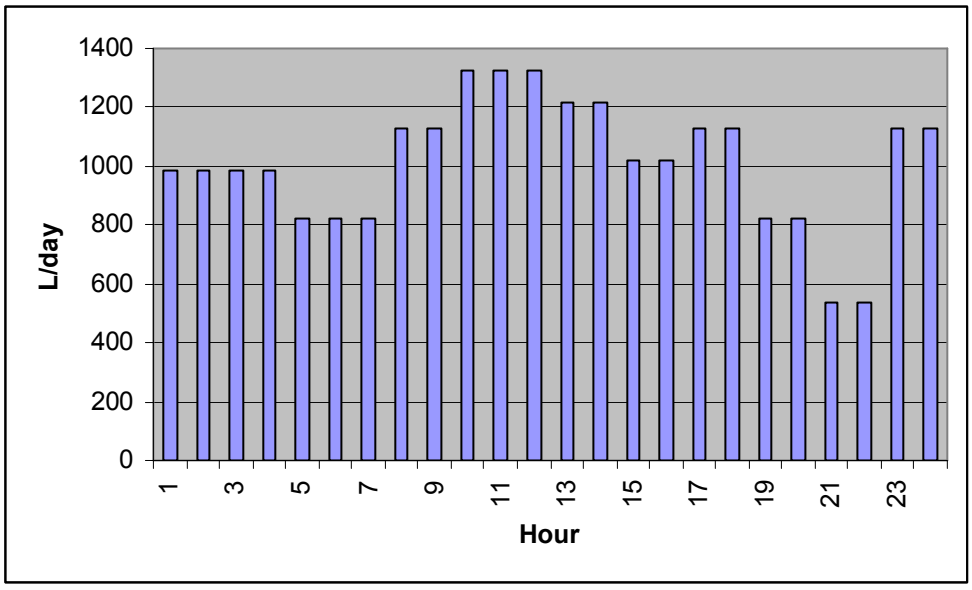

Figure 4.3: Water demand chart

Pump run intervals for each hour of the day are derived from the demand chart. For example, the associated pump operation interval for the hours 0 to 3 are as follows. Given that the product pump delivers 8.4 L/m, or 0.14 L/s:

$$\frac{24hrs \times 60\,\text{min} \times 60\,\text{sec}}{987 Litres / day} \times (0.14 Litres \times 20\,\text{sec}) \approx 245\,\text{sec}$$

Thus the product pump is run every 245 seconds for 20 seconds.

The hour of the day is kept in a reserved register in the PLC (V7770). In rungs 66 to 75, for each hour of the day (0 to 23) a different pump run interval is set in the interval counter according to the demand simulation chart.

4.3 HMI Pages & Configuration

Toggle control also known as on and off control is the most commonly used

4.3.1 I/O Configuration

To provide data for the operator interface pages, Citect uses the concept of an I/O server. The I/O server is responsible for communicating with the I/O devices (such as the PLC), and defining the means of the data exchange (such as communication protocols of different layers). The boards, ports and I/O devices associated to this server must be detailed and parameterised. These parameters can be found in Appendix B. The specific I/O points to be read and/or written to in the PLC can be defined in the Variable Tags table. This variable table specifies the address of each variable, along with its type, units, scaling (if not a digital variable), display format, and defines a tag for the Citect HMI interface pages to refer to.

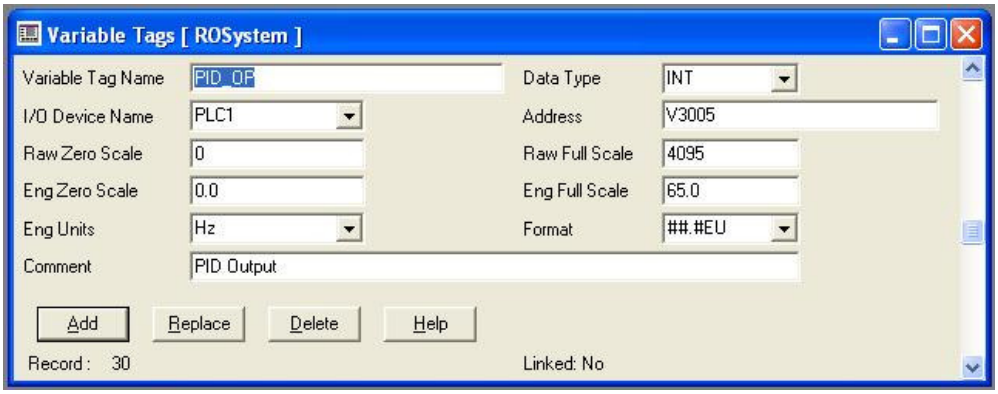

Figure 4.4: Citect variable tags

4.3.2 Overview Page

The aforementioned tags are then used in a HMI page such as the overview page shown below.

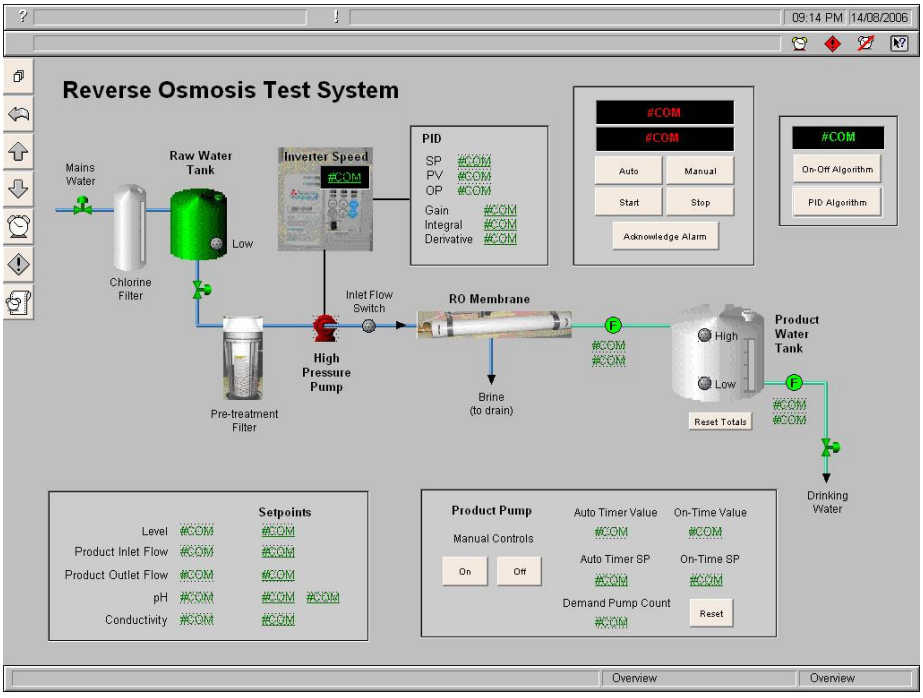

Figure 4.5: Overview page

Each digital dynamic display and each analog value shown on this page was defined in the variable table, and the I/O server scanning the PLC for the specified addresses continually refreshes all these variables. For example, the PID output value, shown on the Overview page as OP in the PID box, would use the tag 'PID_OP' that was previously defined in the variable table (see figure 4.4).

4.3.3 Trends & Alarm Pages

Trends and digital alarms can also be defined in Citect by defining them in the Trend Tags table and the Digital Alarms table respectively. They refer to variables that should already be defined in the Variable Tags table.

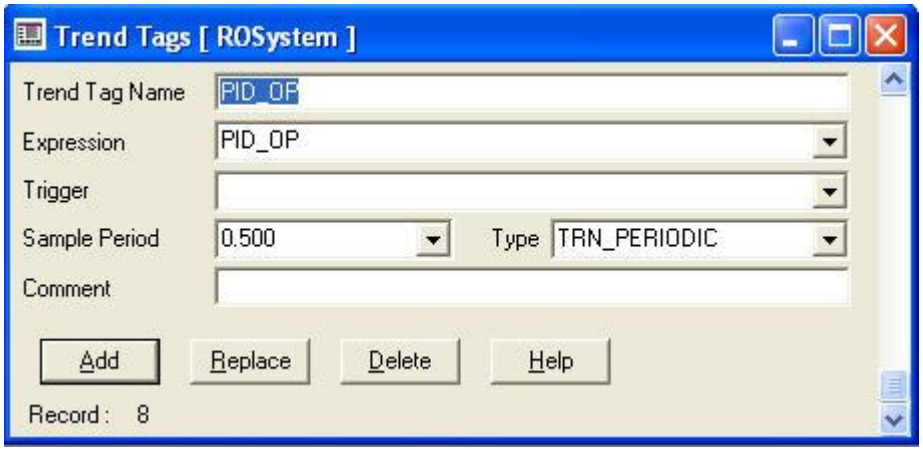

Figure 4.6: Trend Tags

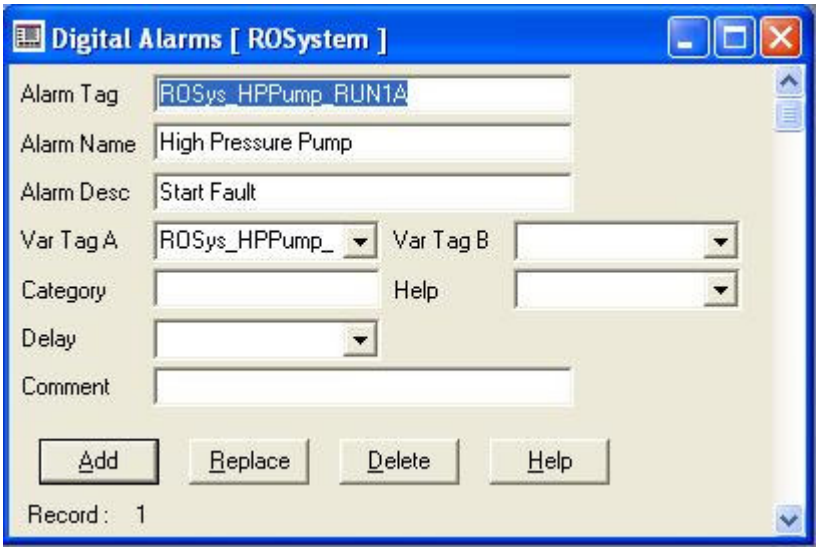

Figure 4.7: Digital Alarms

Citect can create default trends and alarms pages for a project, which refer to tags defined in their respective tables. Note that the computer must be setup as a Trends server for trends to be created.

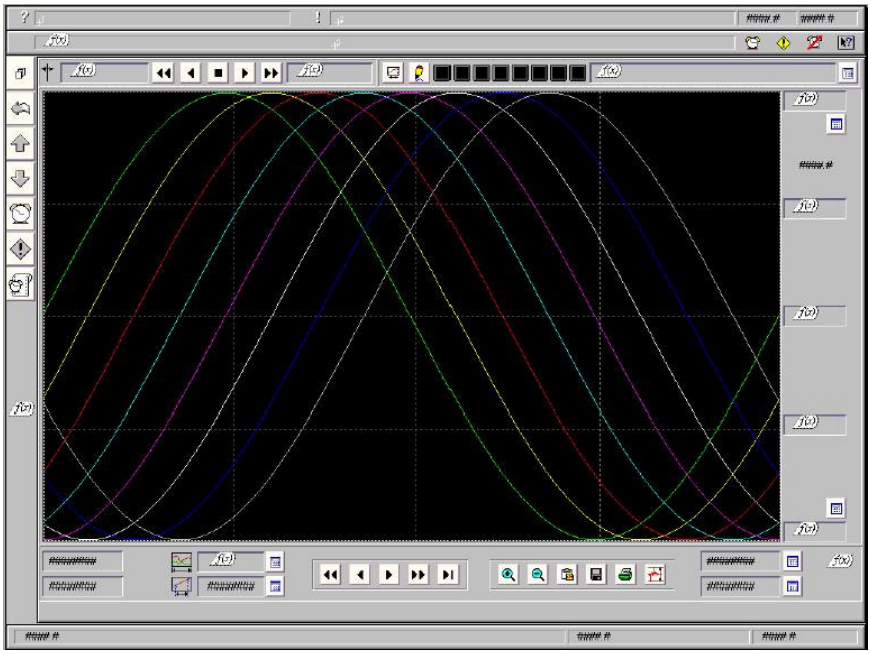

Figure 4.8: Trends page

Figure 4.9: Alarms page

5 SYSTEM MODELING

Mathematically modeling a real-world system can aid in predicting a system's behaviour and/or performance in responding to various input conditions. When a system is accurately modeled, process refinement and performance optimisation may be achieved in the computer-aided mathematical realm, thereby reducing the time consuming and potentially costly reliance on real-world trial-and-error style of optimisation. This type of mathematical modeling can be facilitated by specialized computer software.

Matlab is one such mathematical modeling software that is widely used in engineering research projects across many industries. System models can be created in Matlab and simulated using Simulink, a model simulation application included in the Matlab suite. Simulink provides a graphical user interface that uses various types of elements (blocks) to create a simulation of a dynamic system; i.e. a system that can be modeled with differential or different equations whose independent variable is time.

The reverse-osmosis system is broken down smaller components, which are modeled separately. The component models interact with each other and together represent the whole system. The purpose of modeling the components was to determine their characteristics within the expected range of operation of each component during the operation of the system. The components were tested and the models established for operation within the testing range. The following models are not guaranteed to work outside the testing range and although this approach may limit the applicability of the models in other applications, it was found to be satisfactory in the scope of this work.

The following system models will focus on the overall system's power consumption using different control strategies; hence component models are designed from this perspective.

Note also that earlier in the project, mathematical modeling of the system from textbook formulae was attempted, and these can be found in Appendix F.

5.1 Modeling Method

Some of the component models were derived from experimental data. Where only two variables were involved, Matlab's polyfit function was used to determine the complex polynomial relationships between the variables.

In models where more than two variables are involved, another Matlab function called "Linear-in-the-parameters Multiple Regression" was used in addition to the polyfit function. It consists of a data regression routine, which fits the data points to a predefined non-linear relationship, through least-squares error minimization. To calculate the co-efficients of a predefined non-linear model, a further deduction is needed. For instance, to calculate the relationship between an output variable Y_1, and two input variables, X_1 and X_2, the following non-linear model (linear-in-the-parameters) can be defined:

$$Y = f(X_1, X_2) = k_1 + k_2 X_1^n X_x^n + k_3 X_1^{n-1} X_x^{n-1} + \cdots\cdots + k_{n-1} X_1 X_2 \qquad (5.1)$$

Where

Y_1 is the model output variable;

X_1 and X_2 are the variables used as the model inputs.

For example, in the RO system, let the inlet flow of the product tank be the output variable Y_1, the supply power frequency is X_2, and the salinity of the feed water is X_1. At first, the supply power frequency can be plotted against the output variable by using the polyfit function. This is carried out for different water salinities, yielding a set of polynomial equations. The co-efficients of these equations are compared to those generated from the original experimental data set, which is equal to the desired non-linear terms. The RMS error between the original data and the model fit would be calculated, and if needed, the target non-linear relationship adjusted, giving a different target equation. An RMS error of less than 5% was used as a guideline for the suitability of the data fitting. This tolerance was obtained for most of the derived models.

Another guideline used was the overestimated system warning that Matlab would produce if the data matrix were rank deficient, i.e. if it did not have linearly independent columns. This indicated that the established non-linear model was not suitable and a different target matrix would be chosen.

A printout of the RO system Matlab model is found in Appendix C. All page references in this section refer to this appendix. The layout of the whole RO system is shown in page 1 of Appendix C. The following sections will detail the individual models that make up this system 'container' model. Total energy consumption and water productivity displays were used as real-time indicators, which can be monitored over the simulation period.

5.2 Power Consumption Calculation

The system power consumption model represents the amount of energy used at different frequencies and feed water salinities. By monitoring the energy consumption (kW) over the motor frequency range (20-65Hz) at different feed

water salinities, test data was collected. The polyfit function is used to determine a model polynomial equation from the test data for each salinity level.

The model is found in page 6. Note the different derived functions used to calculate power consumption at different feed water salinities. The motor frequency and salinity level is input into this model to determine the power consumption response of the system. During simulation, the salinity level is fixed and the motor frequency varies as dictated by the selected control strategy.

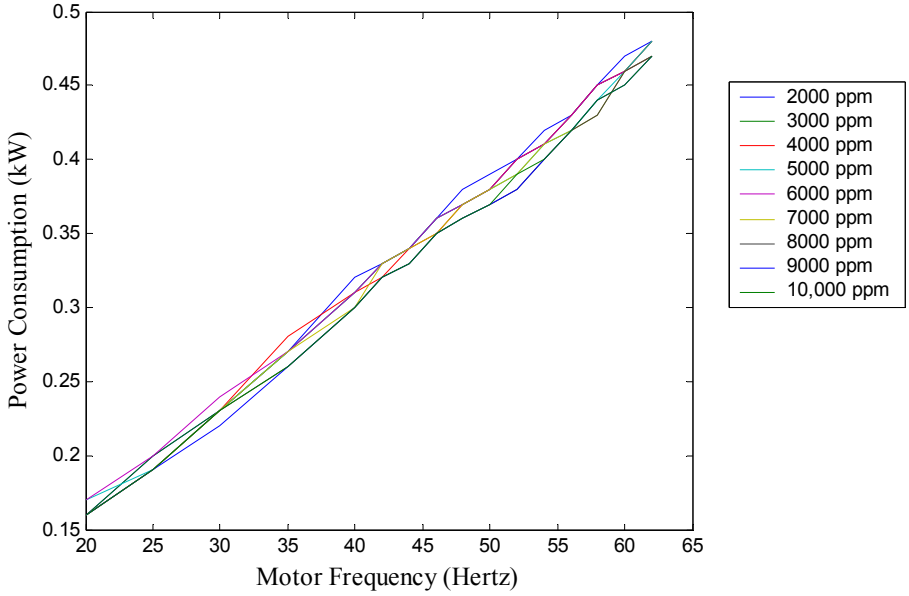

Figure 5.1: Test Data of Power Consumption vs. Frequency

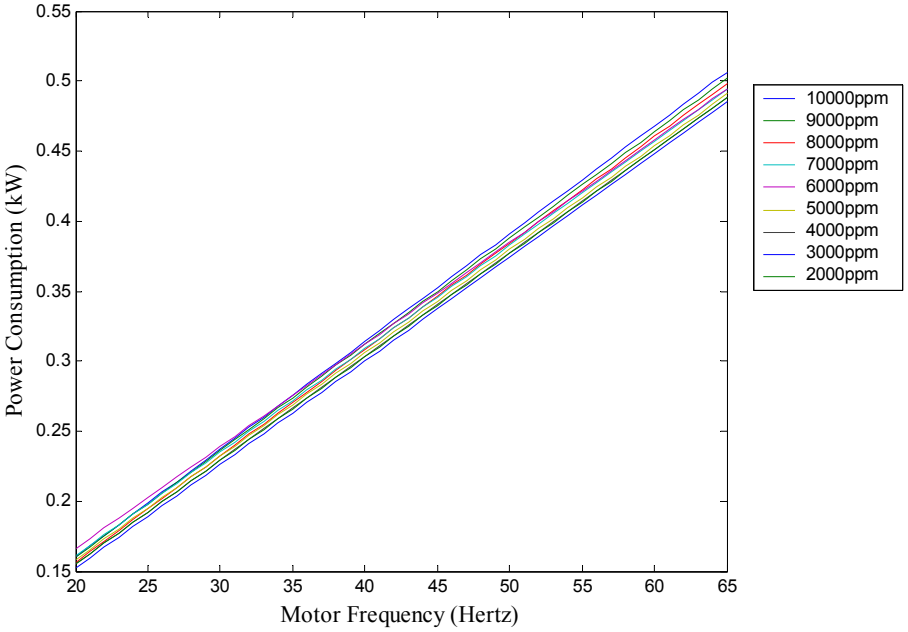

Figure 5.2: Simulated data of Power Consumption vs. Frequency

5.2.1 Feed Water Salinity

The Total Dissolved Solids (TDS) in a liquid, which is measured in parts-per-million or ppm, can represent feed water salinity. Practically however, salt concentration in a liquid is more accurately measured as electrical conductivity, measured in milliSiemens-per-centimeter or mS/cm. The relationship between the two measurements is linear, as shown in the following equation:

$$\text{TDS (ppm)} * 0.64 = \text{Electrical Conductivity (mS/cm)} \quad (5.2)$$

Salt concentration measurements may be obtained using a conductivity meter, and converted to its TDS value.

Fresh water	less than 1,000ppm
Slightly saline water	from 1,000ppm to 3,000ppm
Moderately saline water	from 3,000ppm to 10,000ppm
Highly saline water	from 10,000ppm to 35,000ppm
Ocean water	35,000ppm of salt

Table 5.1: Comparative Salt Concentrations

The above table shows some common salt concentration levels. Note that this RO system is designed for desalinating brackish water whose salt concentration range from 2,000ppm to 10,000ppm.

Saltwater is simulated in this project by adding pool salt into carbon-filtered tap water. The salt water solution is produced using the following equation:

$$ppm = (mg_{salt} / L_{water}) \quad (5.3)$$

Thus to produce a 2000ppm solution you would require 2000 milligrams of salt per litre of water or 2g/L.

5.3 Reverse Osmosis Membrane

Experimental data was gathered via preliminary testing for entry as parameters into the data-fitting Matlab functions. The 3-D plot below illustrates the relationships between permeate flow, motor frequency and feed water salinity.

The following equation is to be used to represent the membrane model.

$$M_p = k_1 X_1^3 + k_2 X_1^2 + k_3 X_1 + k_4 X_f + k_5 \quad (5.4)$$

Where

M_p is the permeate flow rate;

X_1 is the motor frequency;

X_f is the feed water salinity;

k_1, k_2, k_3, k_4, k_5 are the co-efficients of the variables.

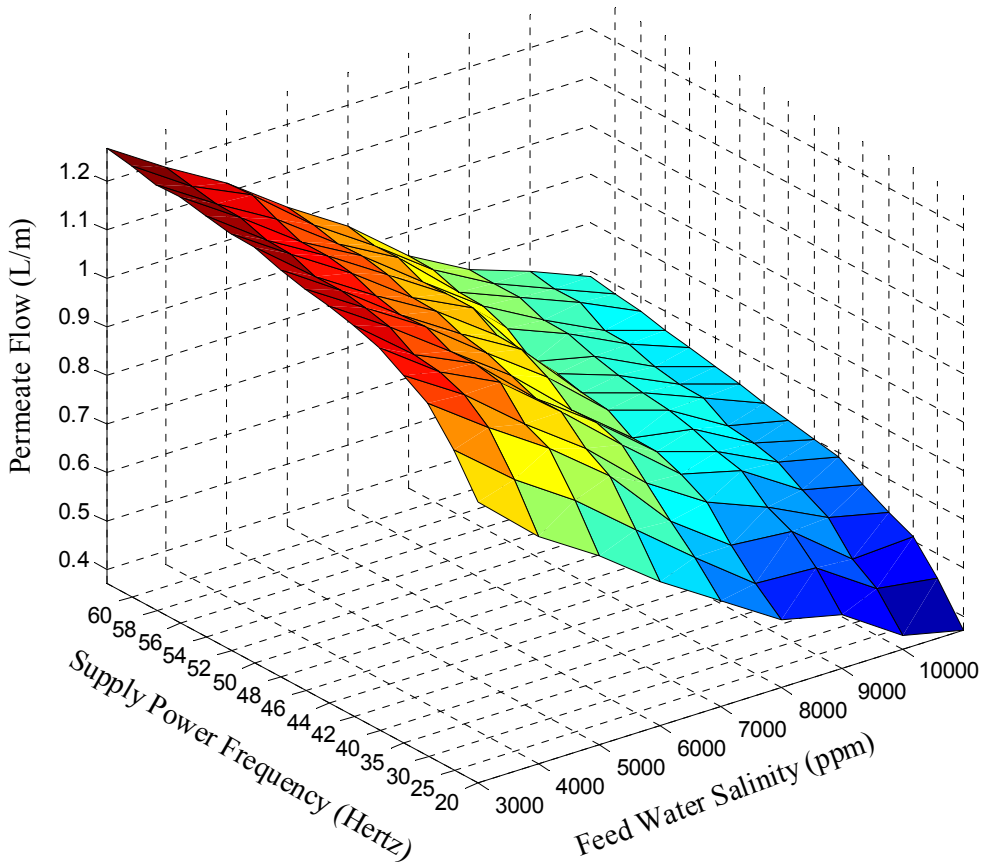

Figure 5.3: Permeate Flow vs. Motor Frequency vs. Feed Water Salinity

From the characteristics of the membrane revealed in figure 5.3, by using the polyfit function in Matlab, the relationship between the motor frequency and permeate flow is approximated at various feed water salinities. As a result, the values of coefficients k_1, k_2, k_3, k_4 and k_5 were determined. For the data-fitting the RMS error was kept to a minimum, and the mean values of k_1, k_2, k_3, k_4 and k_5 were selected, yielding the following equation:

$$M_p = 0.0002X_1^3 - 0.0037X_1^2 + 0.0824X_1 - 0.000071X_2 + 0.98 \qquad (5.5)$$

The above equation is represented in a model, which found on page 18. The simulated results of the model are shown below.

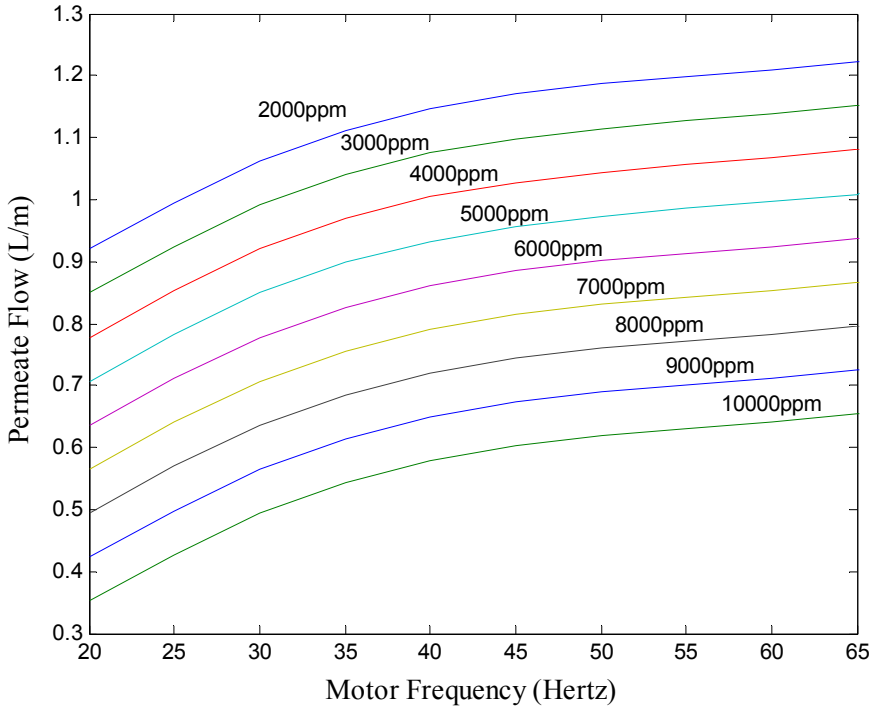

Figure 5.4: Simulation Result of the RO Membrane Model

5.4 PID Control

The PID control model can be found page 4. The main block of this model is the PID controller. The process variable input of the controller is the difference between the inlet and outlet flows of the product water tank. An auto-switch directs the output of the PID controller to the model output when the product water tank is not full. When the product water tank is full, it is set to a low value.

The PID controller is a ready-made function block from the Matlab blocks catalog. The block was modified to include scaling, a starting frequency and output limits, as shown on page 5. The resulting block produces a frequency output with a range of 20Hz to 65Hz.

5.4.1 Start-up of the motor

The starting current of a motor can be 6 to 8 times the rated current of the motor. If large currents are drawn even for a short time, the current rating required of the inverter will become unacceptably large.

At starting, the rotor speed N_m is zero, and hence the slip speed N_{slip} equals the synchronous speed N_{syn}. Therefore, at start-up, a low line frequency must be applied in order to keep N_{slip} low, and hence avoid large starting currents.

Assume that a starting torque of 150 percent of rated is required in order to overcome the starting friction. For a 4-pole AC induction motor at 50Hz supply frequency, the synchronous speed N_{syn} is:

$$N_{syn} = \frac{f \times 60}{(p/2)} = \frac{50 \times 60}{(4/2)} = 1500 \text{ rpm}$$

Given that the rated motor speed N_{rated} =1345 rpm

$N_{rated,slip} = N_{syn} - N_{rated} = 1500 - 1345 = 155$ rpm

At start-up, the rate slip speed of the motor is:

$$1.5 \times N_{rate,slip} = 155 \times 1.5 = 232.5 \text{ rpm}$$

Hence the start-up frequency would be:

$$f_{start} = (\frac{N_{syn,start}}{60}) \times \frac{p}{2} = \frac{232.5}{60} \times 2 = 7.75 \text{ Hz}$$

A startup frequency setpoint for the motor must be over 7.75Hz to keep the motor from stalling under load. For the system, 20 Hertz was chosen to be the starting frequency for the motor, as a lower start speed would generate much more heat and possibly damage the motor. Also, a lower start frequency increases the possibility of stalling the motor if any unpredictable loading occurs during startup.

5.5 Toggle Control

The toggle control model is shown on page 19. A set-reset flip-flop function block is used to toggle the output frequency. Note that the product water tank capacity input is a value between 0 and 1, representing 0-100% of the product water tank. Two comparators determine whether the water level is below 20% or greater than 80%. A true state of either comparators sets or reset the flip-flop respectively. The output of the flip-flop is input into an auto-switch, which selects either 50Hz or 3Hz respectively. This model effectively outputs an 'on' frequency of 50Hz when the product water tank level is less than 20%, and outputs an 'off' frequency of 3Hz when the product water tank is greater than 80%. The 'off' frequency of 3Hz was chosen due to the fact that the adjoining models require values greater than 0 as an input to function properly.

5.6 Water Demand

Pulse generators were used in the water demand model to simulate the water demand scenario over 24 hours. This model can be found on page 20. The parameters of the pulse generators were set according to the specifications described in section 4.2.6 (Product Pump Control and Demand Simulation). Over the period of a day, the different water demands are invoked by setting different pulse frequencies from the pulse generators. For example, a high water demand is implemented using a high pulse frequency. The pulse generators are input into a 24-input multiport switch, representing each hour of the day. A 24-hour clock is used as the control input of the multiport switch to select which pulse frequency is to be used for a given hour. The total water demands over the simulated period was found to be 1140 litres.

5.7 Product Water Tank

The product water tank model is found in page 16. The inlet water flow total is determined by inputting the inlet water flow rate into an integrator, thereby accumulating a total each second. A similar process is carried out for the water consumption flow total.

The tank is set an initial value of half-full (650L). This value is added to by the inlet water flow total and subtracted by the water consumption flow total.

This value is then divided by the total water capacity of the tank (1300L), to produce a water capacity output value between 0 and 1, which is used as an input by the control models (PID and toggle control).

5.8 System Simulation and Results Analysis

The simulations were carried out using the toggle control mode initially, and then the PID control mode. Simulation times in both control modes were set to be 24 hours, which equals to 86400 seconds. The feed water salinity was chosen to be in a span of 2000 to 10,000 with 1000 unit intervals.

The RO system is rated to produce 1000 litres per day, and it was assumed that the water storage could sustain at least one day's usage. The water tank capacity is chosen to be 1300 litres. The initial water volume is 650 litres which is half of the total capacity of the tank.

A series of plots (see figures 5.5 to 5.10) were produced from the simulation results, comparing the performances between the two control strategies, PID and toggle control. A quick scan of these plots revealed that the overall performance of the PID control strategy was superior to the toggle control strategy. The former displayed a savings in energy, an increase in productivity and an improvement in overall efficiency.

Figures 5.5 and 5.6 show that the toggle control strategy shows a rising trend as the feed water salinities increase. This is consistent with the fact that as the feed water salinity rises, more energy is required to produce the same amount of product water. The PID control strategy however, consumes a relatively constant amount of energy despite the variance in feed water salinities.

Figures 5.7 and 5.8 indicate that water productivity decreases for both strategies as the feed water salinities increase, alluding to the fact that the membrane salt rejection limit is near. A greater pressure would be required to maintain the water productivity, but the product quality would decrease as a result.

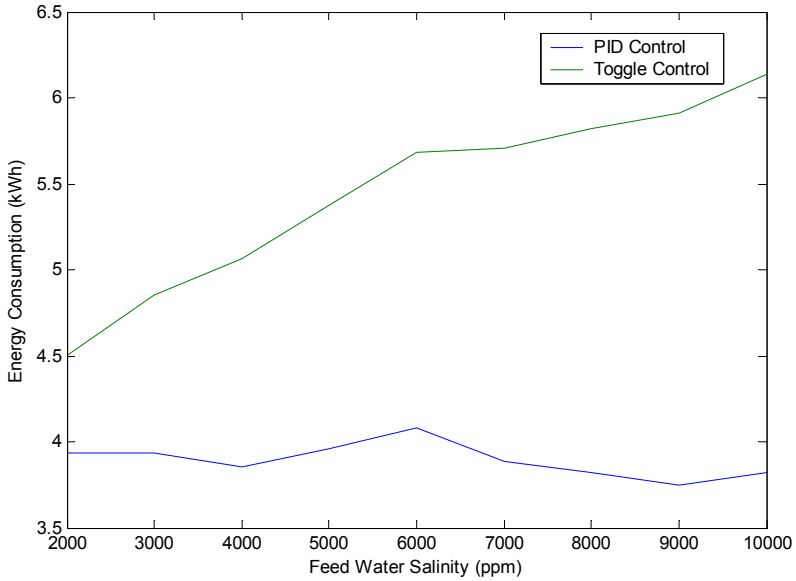

Figure 5.5: Energy Consumption in different feed water salinities

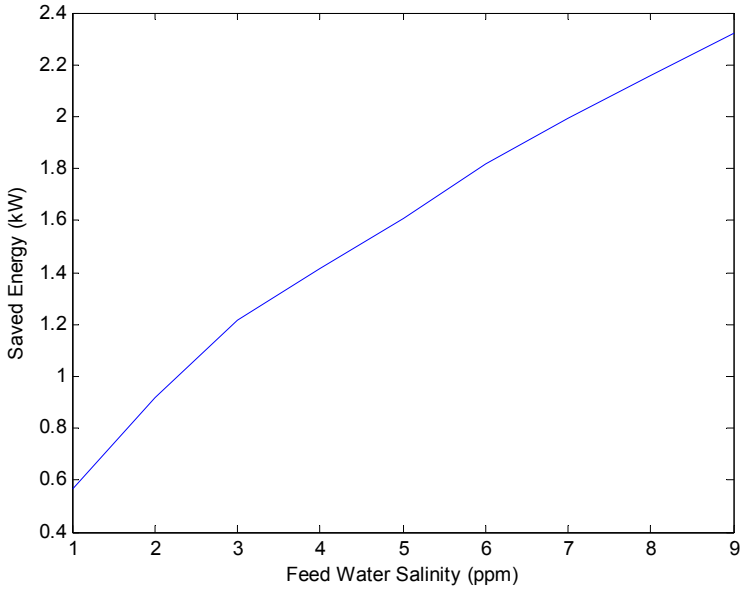

Figure 5.6: Saved energy compared PID control with toggle control

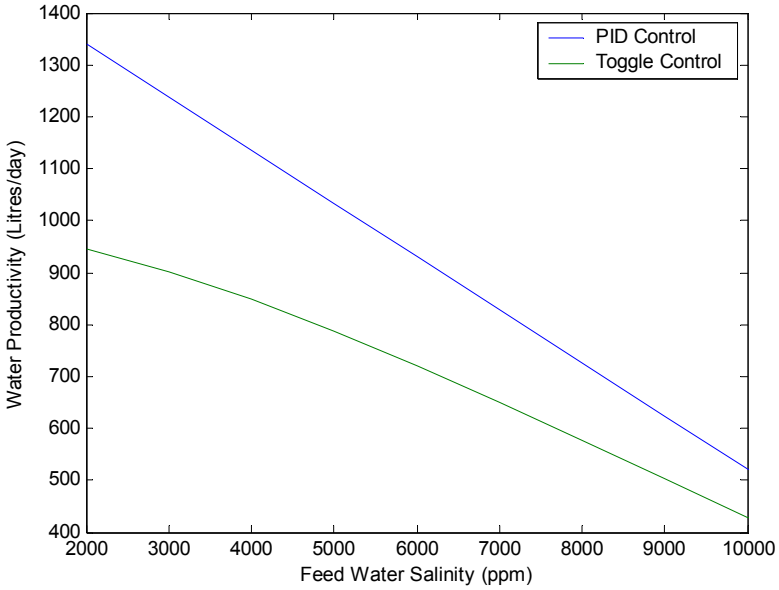

Figure 5.7: Water productivities in different feed water salinities

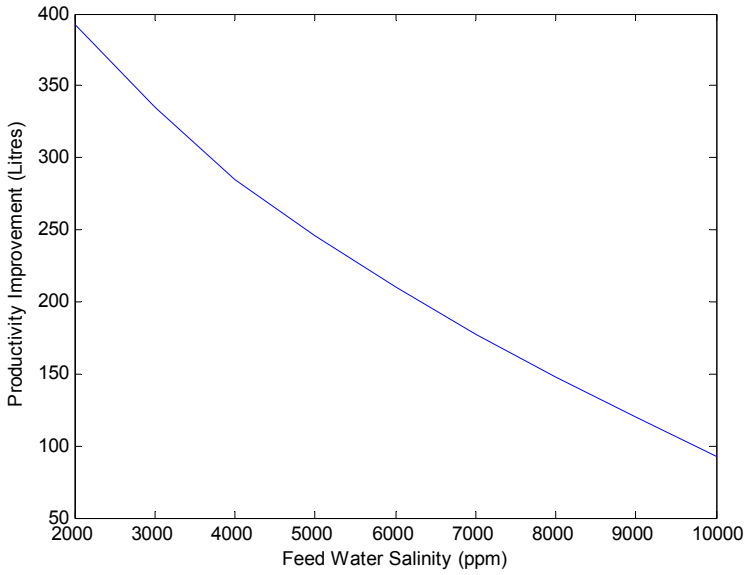

Figure 5.8: Productivity Improvement

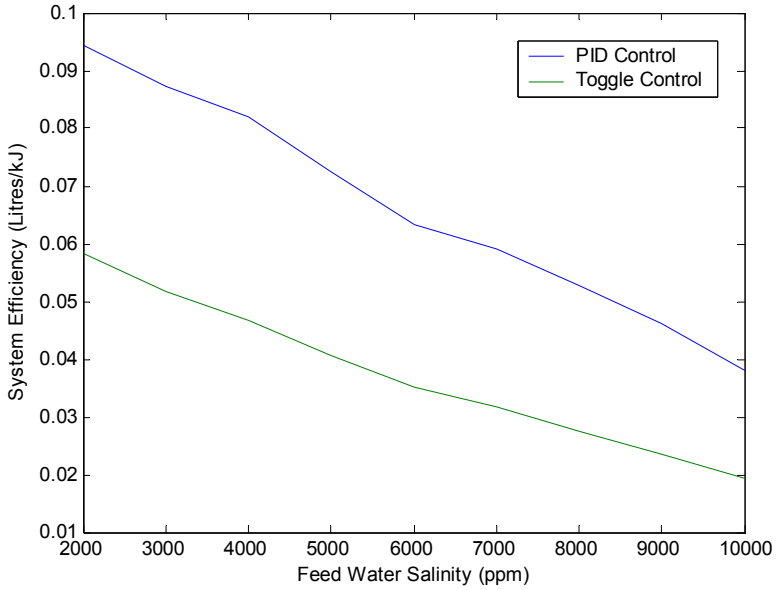

Figure 5.9: System efficiencies in feed water salinities

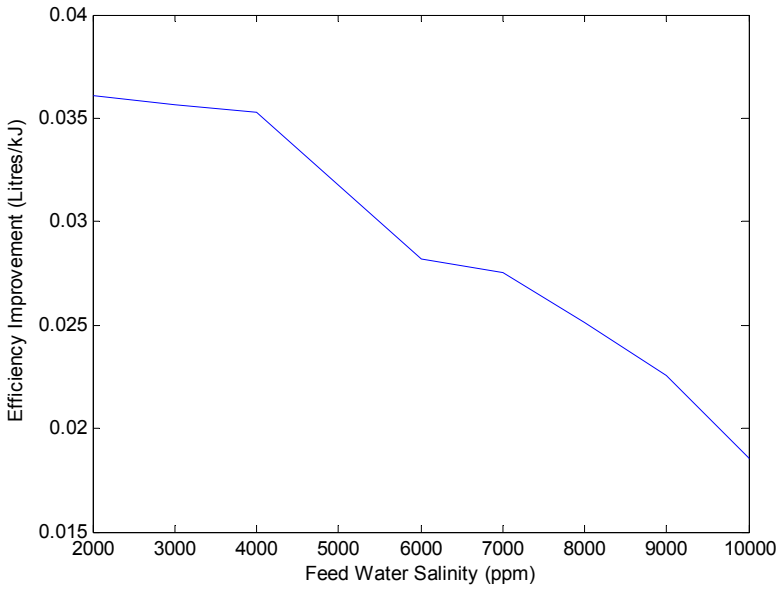

Figure 5.10: Improved system efficiency

6 EXPERIMENTAL METHOD & ANALYSIS

Once the preliminary objective of constructing a reverse-osmosis desalination system was accomplished, the proposed efficiency improvements were applied in turn to the system and tested for improvements in efficiency. A series of experiments were devised and conducted for the respective efficiency improvements.

The first proposal, pump speed control, was integrated into the design of the desalination system; hence experiments were carried out for this efficiency improvement.

Experiments for the second proposal, feed water heating, were also carried out. However, due to time restrictions, these tests were not as extensive as desired.

The third proposal, vacuum pump based energy recovery, was not implemented in this project. This is due to three major factors. The first factor was the fact that the system was too small to recover any substantial energy from - and the expense would not have justified the energy recovered. The second factor was the fact that such a device may need to be fabricated, and before embarking on such a task further study needs to be done on this method's feasibility and effectiveness. The third factor was the time restriction in the project.

For the first two proposals, experimental data was plotted and can be found in Appendix D. All references in this chapter can be found in Appendix D.

6.1 Pump Speed Control

6.1.1 Short Term Performance

A short-term performance test was devised to monitor the correct operation of the system and to observe any energy consumption differences between control strategies at such short intervals. These tests range between 16 to 24 minutes in length. The system's power consumption is recorded using the energy consumption meter (see 3.3.4).

There were two main experiments at different salt concentrations, the first at 2000ppm and the second at 3000ppm. Each experiment tested the performance of the two control strategies separately. Test parameters were recorded for each test, such as the operation mode of the controller, temperature and conductivity of the feed water, parameters of PID loop, test length, and the average power consumption. The flow rates of the product water tank, frequency setpoint and the power consumption were trended by the HMI and the energy meter respectively.

Some parameters are common in both experiments. They include the water demand simulation, where the product water pump runs for 10 seconds every 5 minutes; the start-up level of the product tank, which is 1.5 litres, and the stop level, which is 18 litres.

Note also that the values that were trended by the HMI have the following ranges: product tank inlet flow (pink trend), 0.0 to 1.6L/min; product tank outlet flow (blue trend), 0.0 to 7L/min; and frequency setpoint (green trend), 0 to 65Hz. Hence the HMI trends that are shown in Appendix D (Figures D.2, D.4, D.6 and D.8) are of unrelated magnitude scales, but occurring at the same time scale. They are plotted together essentially to show their trend behaviour.

6.1.1.1 Short Term Performance Experiment 1

The first experiment was conducted at a feed water salt concentration of 2000ppm, first using the toggle control, and then the PID control.

6.1.1.1.1 Experiment 1 Toggle Control Test

As shown in Figure D.1, the power consumption trend accurately reflects the toggle control philosophy by switching on the pump at 50Hz until the product tank high-level is reached (which was not achieved in the duration of this test). The consumed power increased from 0.0 to 0.37kW and stays fairly constant for the remainder of the test. Running for approximately 16 minutes, the average power was 0.37kW and the resulting total energy consumption was 355.2kJ.

In the HMI trend in Figure D.2, note the flat value of the frequency setpoint (green trend), as it is fixed at 50Hz. Similar to the power consumption trend, the inlet flow into the tank (pink trend) also increased from 0.0 to 1.3L/min before settling at approximately 1.2L/min for the remainder of the test.

The spikes that occur on the blue trend every five minutes represent the product tank outlet flow. Note that the outlet flow does not affect the inlet flow, which is controlled by a fixed setpoint.

6.1.1.1.2 Experiment 1 PID Control Test

In this test a PID controller controls the pump speed, or frequency setpoint. It was observed that the power consumption trend rises sharply in response to an outlet flow from the product tank; when the outlet flow stops, the pump is slowed down gradually. This occurs each time the product pump is started, which was started 3 times in this test as is apparent in Figure D.3. The consumed power starts at 0.17kW at the start of the test, denoting the fact that with the PID control strategy, the lowest frequency setpoint is 20Hz. When the product pump was started the power consumption peaks at around 0.36kW and proceeded to

decrease in a linear fashion back to 0.17kW. Running for approximately 21 minutes, the average power was 0.22kW and the resulting total energy consumption was 277.2kJ.

In the HMI trend in Figure D.4, the frequency setpoint (green trend) started at 20Hz, and when the system is started, the inlet flow into the tank (pink trend) rose from 0.0 to 1.1L/min before settling at approximately 1.0L/min. Each time the product pump is started, the frequency setpoint increased sharply to 65Hz and then started to drop relatively linearly back to 20Hz. Similarly, the inlet flow increased sharply to 1.3L/min and then started to fall back to 1.0L/min.

6.1.1.2 Short Term Performance Experiment 2

The second experiment was conducted at a feed water salt concentration of 3000ppm, first using the toggle control, and then the PID control.

6.1.1.2.1 Experiment 2 Toggle Control Test

Figure D.5 showed very similar characteristics to the toggle control test of the previous experiment. Running for approximately 19 minutes, the average power was 0.37kW and the resulting total energy consumption was 392.0kJ.

The same is the case for the HMI trend in Figure D.6, where the frequency setpoint (green trend), is fixed at 50Hz and the inlet flow into the tank (pink trend) increased from 0.0 to 1.3L/min before settling at approximately 1.2L/min for the remainder of the test.

6.1.1.2.2 Experiment 2 PID Control Test

In Figure D.7, the consumed power starts at 0.16kW at the start of the test, corresponding to the lowest frequency setpoint of 20Hz. When the product pump was started the power consumption rose and peaked around 0.35kW and proceeded to decrease in a linear fashion back to 0.16kW. Running for

approximately 24 minutes, the average power was 0.23kW and the resulting total energy consumption was 324.3kJ.

In the HMI trend in Figure D.4, the frequency setpoint (green trend) starts at 20Hz, and when the system is started, the inlet flow into the tank (pink trend) rises from 0.0 to settle at approximately 1.0L/min. Each time the product pump is started, the frequency setpoint increased to 65Hz and then starts to drop relatively linearly back to 20Hz. Similarly, the inlet flow increased to 1.3L/min and then started to drop back to 1.0L/min.

6.1.1.3 Results Analysis & Discussion

The following table presents the results for efficiency analysis. In hindsight, it would have been easier for efficiency analysis if the tests were all of the same duration of 20 minutes; and in addition a product water total for the duration of the test. However, a rough product water total was calculated using the product tank inlet flow trends.

Experiment	Duration	Energy	Product	Efficiency
2000ppm, Toggle	16 min	355.2kJ	19.2L	0.054L/kJ
2000ppm, PID	21 min	277.2kJ	22.8L	0.082L/kJ
3000ppm, Toggle	19 min	392.0kJ	22.8L	0.058L/kJ
3000ppm, PID	24 min	324.3kJ	26.5L	0.081L/kJ

Table 6.1: Experiment Results for Efficiency Analysis

In general, the toggle control strategy consumed more power than the PID control strategy. The efficiency calculation also shows that the PID control strategy produces around 0.025L more water per kJ than the toggle control strategy. However, it was observed that the difference of water being produced at 20Hz (1.0L/min) and 50Hz (1.2L/min) is 0.2L/min. Hence if the test was run

again with the toggle control 'on' frequency set to 20Hz (or some optimized value between 20Hz and 50Hz), the efficiency results may prove interesting.

The resulting trends also show that the difference in production between the tests conducted at 2000ppm and 3000ppm of feed water is negligible at such short durations. The production rates in the respective toggle control and PID control tests were almost identical for both tests. Perhaps a test with much higher salt concentration (such as 10,000ppm) was required in order to observe a decrease in production rate. Or perhaps a very long test (in the order of days or maybe weeks) is required to prove that if the system is run with feed water with a salt concentration of 3000ppm, the membrane would be more prone to fouling and in turn production rates would deteriorate quicker than if the feed water was at 2000ppm of salt concentration.

A significant amount of noise was observed on the inlet flow trend. This is likely to be due to that flow transmitter's low cost and low quality. Some form of filtering in the PLC program could have been done to smooth out the values, but the positive noise generated where there was no flow denotes an offset may also be required.

Gaps in the outlet flow trend were observed each time the product pump was started. These gaps were, in hindsight, due to a trend range programming error. The trend range configured was 0 to 7L/min, whereas it should have been 0 to 16L/min. When the product pump was started, it delivered over 8L/min of flow, greater that the trend range, resulting in the trend gap.

Jagged peaks were observed on the frequency setpoint trend each time the product pump is started. This is due to the large proportional gain applied to a large error. Note that when the product pump is started, the outlet flow is roughly eight times larger than the inlet flow, resulting in a large negative error.

As soon as the product pump stops, the error is significantly reduced, and the PID controller smoothly controls the decrease in frequency.

Comparing the results of this experiment to the simulated results in terms of efficiency as shown in figure 5.9, for toggle control, the simulated efficiencies for feed water salinities of 2000ppm and 3000ppm are 0.059L/kJ and 0.052L/kJ respectively in a decreasing trend; for PID control the efficiencies were 0.094L/kJ and 0.087L/kJ, also in a decreasing trend. The experimental results in table 6.1 reveal a relatively flat trend for both control strategies, and this may be due to the short duration of the tests, as observed earlier. Note that the simulated and experimental values are relatively close at these lower salinity levels; this is expected as the model was derived from actual test data.

6.1.2 24-Hour Performance

Two 24-hour tests were carried out using the demand simulation programmed in the PLC. These tests were devised to monitor the correct operation of the system and to observe any energy consumption differences between control strategies over 24 hours. The system's power consumption is recorded using the energy consumption meter.

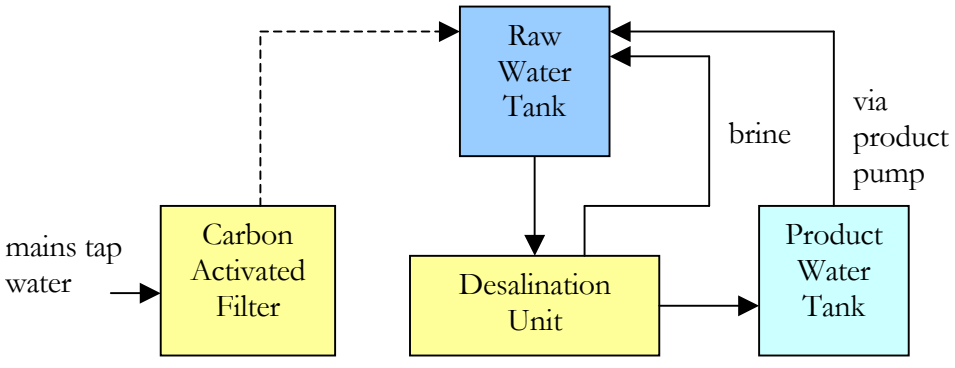

Figure 6.1: 24-hour Test Configuration

As the system runs for 24 hours mostly unsupervised, the test configuration shown on Figure 6.1 was set up.

This configuration was set up primarily to avoid the raw water tank from overflowing, and to conserve the raw water tank's salt concentration. The original setup specified that the raw water tank be filled by water from the mains supply. However, due to the unsupervised duration of these tests, it was decided that the mains water tap be closed (hence the dotted line in Figure 6.1) and for the brine and the demand product water (which is pumped out of the product water tank by the product pump) to be recycled into the raw water tank. This is due to the fact that there is no mechanism to shut off the mains supply in the event of a system failure; and when the system ceases to process water from the raw water tank, the tank would keep being filled and eventually overflow. In addition, it was also thought the recycling and remixing the brine and demand product water in this setup configuration would preserve the controlled salt concentration of the raw water tank.

6.1.2.1 24-Hour Performance - Toggle Control

This test was carried out with a feed water salt concentration of 4000ppm, using the toggle control. In Figure D.11, the power consumption trend reflects the toggle control philosophy by switching on the pump at 50Hz until the product tank high-level is reached. A tank high level was not achieved in the duration of this test, since the system did not appear to stop at all. The consumed power increased from 0.0 to 0.42kW and stays relatively constant for the remainder of the test. The average power was 0.41kW and the resulting total energy consumption was 35427kJ.

In the HMI trend in Figure D.12, it was surprising to see that the expected flat value of the inlet flow into the tank (green trend) was absent. This trend started at

about 0.72L/min after starting and proceeds to drop non-linearly to a low of 0.3L/min, rising and falling again to return to around 0.67L/min, almost exactly 24 hours later.

6.1.2.2 24-Hour Performance - PID Control

This test was carried out with a feed water salt concentration of 4000ppm, using the PID control. It was observed in Figure D.14 that the power consumption trend varies continuously in response to an outlet flow from the product tank. This occurs each time the product pump is started, which was started 352 times over the duration of this test. The consumed power varies between at 0.16kW, the lowest frequency setpoint of 20Hz, and 0.41kW, the highest frequency setpoint of around 50Hz. Figure D.15 shows a zoomed in view of the power consumption trend; the rising and falling of the energy consumption resulting from product pump activity. The average power was 0.23kW and the resulting total energy consumption was 19872kJ.

In the HMI trend in Figure D.16, the inlet flow into the tank (green trend) showed a similar response as that of the toggle control test, but not as pronounced. The inlet flow started at around 0.68L/min and reached its lowest point at 0.36L/min before ending the test 24 hours later at 0.68L/min again. The frequency setpoint trend (red trend) also showed that it generally raised its output from the 6th to the 21st hour of the test.

6.1.2.3 Results Analysis & Discussion

The inlet flow trends of both the 24-hour tests showed unequivocally that gravity plays a large role in the pressure generation of the system and hence the resulting permeate flow of the membrane. When the raw water tank is full, a larger body of water is pushing down into the system from the raised water tank, creating a large pressure. As this level decreases, so does the pressure proportionally. Ideally the

raw water tank needs to be kept as full as possible, and this can be done by having a high level switch in the tank to control an actuated valve at the mains water tap.

The idea of preserving the raw water tank salt concentration was proven to be unsound by the test results. This is due to the fact that the more product water is retained in the product water tank, the higher the salt concentration becomes in the raw water tank. The demand-controlled product pump is the only provider of low-concentration water back into the raw water tank, whereas the brine is continuously fed back into the water tank as long as the system is running.

It was also observed that there were different concentration areas in the raw water tank when measuring the conductivity of the recycled brine and product water. A mixer can be installed in the raw water tank to effectively mix of the recycled brine and product water.

Another issue with this test setup is the lack of a flow totalising unit at the outlet of the membrane. Totalising using the PLC via the flow meter readings have proved inaccurate and unreliable. As a result the total water produced from the system was not monitored in this test. In turn, this meant that the efficiency of the system over the test period could not be performed.

6.2 Feed Water Heating

Two tests were carried out to determine the effect of feed water heating on the system's productivity. Along with the permeate flow, the brine flow was monitored using flow transmitters. Both tests were carried out at a salt concentration of 2000ppm. The first test was carried out at 22.7^0C and the second at 31.5^0C. Records were taken at 40Hz, 50Hz and 64Hz.

It was observed when comparing Table D.5 and D.6 that the membranes permeate flow rate was consistently and significantly (by 0.4L/min) higher in the tests carried out at 31.5^{0}C than those at 22.7^{0}C. However, the brine flow rates were also higher. It may possibly be that a component of the higher flow was due to gravity, which suggests that the raw water tank level was higher for the tests at 31.5^{0}C than the level for the tests at 22.7^{0}C.

The instantaneous power recorded for the 64Hz tests. The 22.7^{0}C test was higher at 772.9W compared to the 31.5^{0}C test at 725.1W. This result suggested that the inverter had to work harder for the 22.7^{0}C to achieve the requested frequency setpoint than for the 31.5^{0}C test. This could also be either due gravity or the decreased viscosity of the liquid at higher temperatures.

A table to show the proportion of permeate flow compared to brine flow is created in an attempt to reveal the actual effect of the different temperatures.

Temperature (^{0}C)	Frequency (hz)	Permeate Flow (L/min)	Brine Flow (L/min)	Proportion of Permeate (%)
22.7	40	1.10	8.39	0.12
22.7	50	1.15	10.21	0.10
22.7	64	1.22	15.11	0.07
31.5	40	1.49	8.90	0.14
31.5	50	1.53	11.12	0.12
31.5	64	1.61	16.42	0.09

Figure 6.2: Permeate Flow vs. Brine Flow

Again it seems that at the higher temperature, there is a slightly higher permeate flow. But these results are inconclusive, and the effect of gravity still cannot be

ruled out. The tests need to record the level of the water tank to be entirely sure that gravity is not playing a part in the increased productivity.

7 CONCLUSION

Reverse-osmosis as a desalination technique is well established; today we are seeing more reverse-osmosis based desalination plants being built around the world where the expected water demand has exceeded the available resource. But this comes at a cost; large high-pressure pumps that push large bodies of saline solutions through a myriad of reverse-osmosis racks require a great amount of energy, mainly from the fossil fuel fed grid. Such is the dependency on a non-renewable resource that is fast diminishing, that there is a justifiable urgency for the requirement for renewable resources to occupy the inevitable void. But the technology of renewable resources is still in relative infancy, and to meet the needs of modern industrial and domestic power requirements using renewable energies are still deemed as fanciful or futuristic.

However, the gap between now and the idealistic 'then' can be lessened not only by creating new technologies for renewable energies, but also by reducing the general power consumption. If such powered devices were to be modified to be more efficient and consume less power without any loss in performance, the said gap can be reduced from both ends.

This research project was embarked on with this perspective in mind. A review of the project is presented below, along with recommendations for the future research.

7.1 Review of the Project

7.1.1 System Construction

The construction and subsequent operation of the system was viewed as a considerable achievement. The simple design of the system may appear to be reasonably straightforward to assemble, but in practice it was the sourcing of the system components that proved to be the main challenge.

The acquisition of project equipment using limited financial resources is synonymous with university projects, and this project was no exception. The university kindly funded the purchase of the high-pressure motor and pump, reverse-osmosis membrane and the flow transmitters. The remainder of the equipment were either loaned by the Electrical Laboratory, loaned or donated by members of the engineering industry, or purchased by the students.

The Curtin Electrical Laboratory was most helpful in providing equipment and technical support. They made available for use the inverter, frequency converters, 24V DC power supply, HMI PC, power meter, miscellaneous electrical equipment, tanks, level switches, and piping. The Curtin Chemistry Laboratory made available the conductivity and temperature meter.

The students also contacted industry members (engineering suppliers and consultants) for the possibility of equipment loan or donation to the project. Bloch Technologies donated the PLC and HMI software. The PLC itself was donated in whole, priced at approximately AUD2,500, by Tenix Alliance. Endress and Hauser also temporarily loaned a conductivity meter to the project.

The limited funding also obliged the students to be creatively resourceful; an exceptional case was the sourcing of the voltage to current signal conditioner.

The requirement was for a frequency to voltage converter to be interfaced to a 4-20mA analog input card on the PLC. Off-the-shelf voltage to current signal conditioners costs upwards of AUD500. However, the students were able to source a voltage to current converting IC chip on-line (US eBay), which was subsequently tested on a breadboard and then finally onto perfboard for the final installation.

The resulting system proved to be quite robust, in its core functions of system process monitoring and the control of the high-pressure and demand pumps. Once the hardware was assembled and the control system was programmed, the system performed quite reliably without much modification required. This was attributed to the simplicity of the design and the quality of the components.

7.1.2 System Modeling

The system was modeled from an energy consumption perspective. Empirical results with an energy consumption orientation were collected from preliminary tests on the system. These results were entered into Matlab, utilising its curve fitting functions to derive the transfer functions for those system components. Logical components were also modeled to represent PLC logic, such as the PID controller and demand logic.

The resulting simulations compared the power consumptions of two control strategies, with the PID control strategy proving more energy efficient that the toggle control strategy.

Note that the efficiency improvement proposal concerning the control strategies were inherent in the design of the system, and was consequently modeled. The other efficiency improvement proposals were not however. Whereas the vacuum pump proposal was deemed outside the scope of this project, tests for the feed

water heating proposal could have been conducted for modeling. Unfortunately, this was carried out much later in the project, and was not modeled.

7.1.3 Efficiency Improvements

The first efficiency improvement proposal, high-pressure pump speed control, was inherent in the design of the constructed system. Hence testing for this proposal was relatively thorough compared to the other proposals. The short-term test results support the proposal that the PID control strategy is more energy efficient than the toggle control strategy. A quick analysis of the power meter trends of the two strategies reveals that the PID controller saves energy by following the load (demand flow). Methods for long-term testing can be improved upon by troubleshooting the issues raised in this project, eg. adding a totalising flow meter at the membrane outlet to determine the system efficiency.

Tests results for the second proposal, feed water heating, showed promise, but the test results were too few to be conclusive. Other factors also raised doubts about the results, and more extensive controlled testing is required. Future projects can concentrate on improving the testing method, and also investigating new methods to heat the feed water using renewable energies.

The third proposal, vacuum pump based energy recovery, was not implemented in this project due to a number of factors, but the idea can be further investigated in future projects.

7.2 Final Comments

Note that whilst the use of the PLC and HMI as the control system provides a convenient test bed that allows easy monitoring and control during testing of the system, it is considered unnecessarily powerful and expensive for a commercial system of this size. Once the concepts are proven, the installed system controller only needs to be large enough to accommodate the I/O required by the system,

and powerful enough to run a single PID controller. This would reduce the cost of the system significantly.

This project can be viewed as an effective springboard for further investigation, not only for improving the efficiency of a small-scale desalination system, but limitless other directions of focus.

7.3 Published Work

This project contributed to the publication of the following work.

1. Rob Susanto-Lee, Yu Zhao, Chem Nayar. *Reverse Osmosis Desalination in an Existing Renewable Energy System.* Proceedings of the IFAC workshop entitled "Energy Saving Control in Plants and Building", Bansko, Bulgaria, 2006, pp241-246.

REFERENCES

Every reasonable effort has been made to acknowledge the owners of copyright material. I would be pleased to hear from any copyright owner who has been omitted or incorrectly acknowledged.

1. Citor Pty Ltd, *"Desalinator Model 1TM Instruction Manual"*, Citor Pty Ltd, 2005

2. D.C. Bullock and W.T. Andrews, "*Deep Sea Reverse-osmosis: The Final Quantum Jump"*. http://www.desalco.bm/d-pdfs/deepsea.pdf, accessed May 2005

3. P.M Wild, G.W. Vickers and N. Djilali, "*The fundamental principles and design considerations for the implementation of centrifugal reverse osmosis*". Proc Instn Mech Engrs, 1997, 211, pp67-81.

4. Nitto Denko, "*ES10 Ultra-low pressure spiral RO element*". http://www.nitto.com/product/datasheet/menbren/003/index.html, accessed May 2005

5. J.P. MacHarg and S.A. McClellan, "*Pressure Exchanger Helps Reduce Energy Costs"*. Journal AWWA, November 2004, pp44-47

6. Spectra Watermachines, "*The Spectra Clark Pump*". http://www.spectrawatermakers.com/, accessed May 2005

7. J.P. MacHarg, **"***The Real Net Energy Transfer Efficiency of an SWRO Energy Recovery Device*". http://www.energy-recovery.com/ tech/real.pdf, accessed May 2005

8. M.S. Miranda, "*Small-scale Wind-Powered Seawater Desalination Without Batteries*". Doctoral Thesis, Loughborough University, UK, 2003

9. A.S.M. Al-Alawi, "*An integrated PV-diesel hybrid water and power supply system for remote arid regions*". Doctoral Thesis, Curtin University, Western Australia, 2004

10. LaTrobe University, "*Model Water Heater*". http://www.latrobe.edu.au/solar/Curriculum Materials/Model Water Heater.pdf, accessed May 2005

11. R.W. Baker, E.L. Cussler, W. Eykamp, W.J. Koros, R.L. Riley, H. Strathman, "*Membrane Separation Systems: recent developments and future directions*". Noyes Data Corporation, 1991

12. M.R. Ladisch, "*Bioseparations engineering: principles, practice, and economics*". John Wiley and Sons, 2001

13. Y. Osada, T. Nakagawa, "*Membrane science and technology*". Marcel Dekker Inc, 1992

14. M.J. Willis, *"Proportional-Integral-Derivative Control"*. MNPERE Minneapolis, Minnesota, 2003

15. N. Mohan, *"Electric Drives - an integrative approach"*. Department of Chemical and Process Engineering, University of Newcastle, 1999

16. P. Rohner, "*PLC: automation with programmable logic controllers*", UNSW Press, Kensington, 1996

17. R.C. Dorf, R.H. Bishop, "*Modern Control Systems"*. Pearson Education Australia, 2005.

18. TECO, "*7200J Inverter-Instruction Manual*", TECO Taiwan, 1987

19. DOW, "*FILMTEC SW30HR-380 Membrane Elements*". http://www.dow.com/liquidseps/pc/jump/filmtec/30hr_380.htm, accessed July 2005

20. Pepperl & Fuchs, *"KFU8-FSSP-1.D Frequency Converter User Manual"*, Pepperl & Fuchs, 2005